

# Frequency-Domain Equalization for Broadband Single-Carrier Multiple Access

Fumiyuki ADACHI<sup>†a)</sup>, Fellow, Hiromichi TOMEBA<sup>†</sup>, and Kazuki TAKEDA<sup>†</sup>, Student Members

**SUMMARY** Single-carrier (SC) multiple access is a promising uplink multiple access technique because of its low peak-to-average power ratio (PAPR) property and high frequency diversity gain that is achievable through simple one-tap frequency-domain equalization (FDE) in a strong frequency-selective channel. The multiple access capability can be obtained by combining either frequency division multiple access (FDMA) or code division multiple access (CDMA) with SC transmission. In this article, we review the recent research on the SC multiple access techniques with one-tap FDE. After introducing the principle of joint FDE/antenna diversity combining, we review various SC multiple access techniques with one-tap FDE, i.e., SC-FDMA, SC-CDMA, block spread CDMA, and delay-time/CDMA.

**key words:** single-carrier, frequency-domain equalization, frequency-selective channel, wireless systems

## 1. Introduction

In the present 3rd generation (3G) wireless networks, direct-sequence code division multiple access (DS-SS) with coherent rake combining [1] is employed. Hereafter, instead of using the terminology “DS-SS,” the terminology “single-carrier CDMA (SC-SS)” is used. Multiple copies of a transmitted signal are received via a multipath channel. A channel having more than one resolvable propagation path is called a frequency-selective channel. In a SC-SS receiver with coherent rake combining, multiple copies of the transmitted signal are recovered through a despreading process and are coherently combined (coherent rake combining). In order to increase the data rate, the chip rate must be increased. Since the delay time resolution of the receiver is inversely proportional to the chip rate. Therefore, as the chip rate increases, the delay time resolution of the receiver improves. As a consequence, the number of resolvable propagation paths increases and the channel becomes a strong frequency-selective channel. This causes a serious problem in that SC-SS with coherent rake combining provides very poor performance because of strong inter-chip interference (ICI) resulting from the presence of an excessive number of propagation paths.

Multi-carrier CDMA (MC-SS) with simple one-tap frequency-domain equalization (FDE) [2]–[4] can take advantage of the channel frequency-selectivity and it has

long been considered as a strong candidate for a broadband multiple access technique. However, quite recently, SC multiple access has been reconsidered as a promising uplink (mobile-to-base) multiple access technique since it has lower peak-to-average power ratio (PAPR) than MC multiple access while achieving a significant performance improvement through simple one-tap FDE in a strong frequency-selective channel [5]–[11].

In this article, we review the recent research on the SC multiple access techniques with one-tap FDE. First, we introduce the principle of joint FDE/antenna diversity combining in Sect. 2. Then, in Sect. 3, we introduce a combination of SC with FDE and FDMA (referred to as SC-FDMA). Section 4 presents how the introduction of FDE significantly improves the performance of conventional SC-SS in a strong frequency-selective channel. However, even if FDE is used in the uplink, multiple access interference (MAI) remains because different users’ signals are received via different channels. This can be remedied by combining SC-SS and FDMA (note that this is equivalent to SC-FDMA combined with a spread spectrum technique). Another promising CDMA technique is block spread CDMA. The principle of block spread CDMA is presented in Sect. 5. A new hybrid SC multiple access technique called delay-time/CDMA is introduced in Sect. 6. Section 7 concludes the paper. Note that throughout this article, ideal channel estimation and no channel coding are assumed for clear understanding of the fundamentals of SC multiple access with one-tap FDE.

## 2. Principle of Joint Frequency-Domain Equalization (FDE)/Antenna Diversity Combining

### 2.1 Model of Broadband Wireless Channel

The channel consists of many distinct propagation paths resulting from reflection and diffraction of the transmitted signal by many obstacles located between a transmitter and a receiver. We assume a block fading channel, i.e., the channel stays unchanged during the transmission period. Assuming  $L$  distinct propagation paths, the channel impulse response,  $h(\tau)$ , between the transmit and receive antennas can be expressed as

$$h(\tau) = \sum_{l=0}^{L-1} h_l \delta(\tau - \tau_l), \quad (1)$$

where  $h_l$  and  $\tau_l$  are the complex valued path gain with

Manuscript received October 10, 2008.

Manuscript revised January 27, 2009.

<sup>†</sup>The authors are with the Department of Electrical and Communication Engineering, Graduate School of Engineering, Tohoku University, Sendai-shi, 980-8579 Japan.

a) E-mail: adachi@ecei.tohoku.ac.jp

DOI: 10.1587/transcom.E92.B.1441

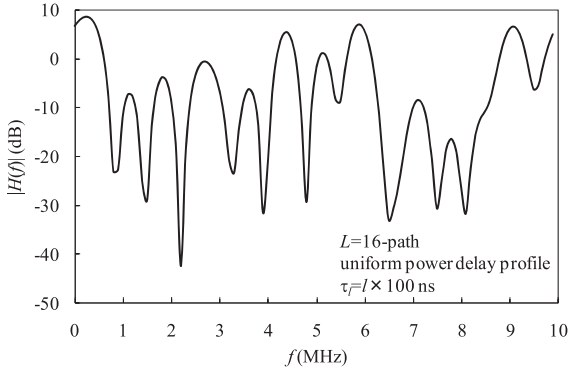


Fig. 1 Broadband channel.

$\sum_{l=0}^{L-1} E[|h_l|^2] = 1$  and the time delay of the  $l$ -th path, respectively, where  $E[\cdot]$  denotes the ensemble average operation.

The channel transfer function (or the channel gain at frequency  $f$ ) is given by

$$H(f) = \sum_{l=0}^{L-1} h_l \exp(-j2\pi f \tau_l). \quad (2)$$

A one shot observation of  $H(f)$  is illustrated in Fig. 1. A frequency-selective channel having an  $L = 16$ -path uniform power delay profile with  $E[|h_l|^2] = 1/L$  and  $\tau_l = l \times 100$  ns (i.e., the  $l$ -th path length in distance is  $l \times 30$  m) is assumed.

Let the transmitted signal spectrum be denoted by  $S(f)$ . As the data rate increases,  $S(f)$  spreads more and therefore,  $H(f)$  changes within the signal bandwidth. Such a channel is called the frequency-selective channel. The received signal spectrum,  $R(f) = S(f)H(f)$ , is distorted in a frequency-selective channel [12]. Thus, the use of advanced equalization techniques is indispensable.

The spectrum distortion can also be understood by observing the time-domain received signal. Non-spread SC transmission is considered. The received signal,  $r(t)$ , at time  $t$  can be expressed using the baseband equivalent representation as

$$r(t) = \sum_{l=0}^{L-1} h_l s(t - \tau_l) + n(t), \quad (3)$$

where  $s(t)$  is the transmitted signal and  $n(t)$  is the additive white Gaussian noise (AWGN). What we can understand from Eq. (3) is that past signals interfere with the present signal, thereby causing severe inter-symbol interference (ISI). Some equalization techniques must be employed to eliminate the ISI and to improve the transmission performance.

## 2.2 Joint FDE/Antenna Diversity Combining

Figure 2 illustrates the transmitter/receiver structure of SC with FDE.  $N_r$  receive antennas are used. SC with FDE is a block transmission. Below, we consider the transmission of a block of  $N_c$  data-modulated symbols. From now onward, we use the discrete-time signal representation with variable

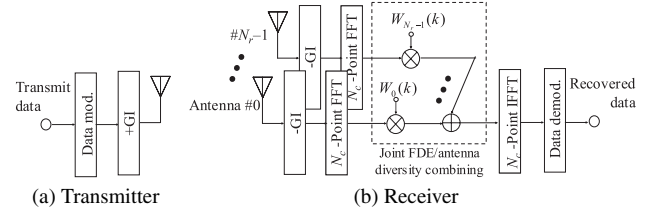


Fig. 2 Transmitter/receiver structure for SC transmission.

$t = (0 \sim (N_c - 1))$  representing the symbol-spaced discrete time.

A signal block,  $\{s(t); t = 0 \sim (N_c - 1)\}$ , is transmitted after inserting an  $N_g$ -sample cyclic prefix (CP) into the guard interval (GI). The GI length should be longer than the maximum time delay difference among the propagation paths. The received signal is expressed using the continuous-time representation as Eq. (3). Due to the CP insertion, the received signal can be a circular convolution of the transmitted signal block and the channel impulse response.

The received signal is sampled at the symbol rate. The received signal block at the  $m$ -th ( $m = 0 \sim (N_r - 1)$ ) receive antenna after removing the GI can be expressed using the matrix form as

$$\begin{aligned} \mathbf{r}_m &= [r_m(0), \dots, r_m(t), \dots, r_m(N_c - 1)]^T \\ &= \mathbf{h}_m \mathbf{s} + \mathbf{n}_m = \sqrt{\frac{2E_s}{T_s}} \mathbf{h}_m \mathbf{d} + \mathbf{n}_m, \end{aligned} \quad (4)$$

where  $(\cdot)^T$  denotes the transpose operation,  $\mathbf{s} = [s(0), \dots, s(t), \dots, s(N_c - 1)]^T$  is the transmit signal vector,  $\mathbf{d} = [d(0), \dots, d(t), \dots, d(N_c - 1)]^T$  is the transmit symbol vector with  $d(t)$  representing the  $t$ -th data-modulated symbol with  $E[|d(t)|^2] = 1$ , and  $E_s$  and  $T_s$  represent the symbol energy and symbol duration, respectively.  $\mathbf{n}_m = [n_m(0), \dots, n_m(t), \dots, n_m(N_c - 1)]^T$  is the noise vector with  $n_m(t)$  representing the noise sample with variance  $2N_0/T_s$ , where  $N_0$  is the AWGN one-sided power spectrum density.  $\mathbf{h}_m$  is the circulant matrix of size  $N_c \times N_c$  representing the channel impulse response given by

$$\mathbf{h}_m = \begin{bmatrix} h_{m,0} & & & h_{m,L-1} \cdots & h_{m,1} \\ h_{m,1} & \ddots & & & \vdots \\ \vdots & \ddots & h_{m,0} & & h_{m,L-1} \\ h_{m,L-1} & h_{m,1} & \ddots & & \\ \vdots & \vdots & \vdots & \ddots & \\ h_{m,L-1} & & h_{m,L-1} & \ddots & h_{m,0} \\ \vdots & & \vdots & \ddots & \vdots \\ \mathbf{0} & & & h_{m,1} & \ddots \\ & & & \vdots & \ddots & h_{m,0} \end{bmatrix}, \quad (5)$$

where  $h_{m,l}$  denotes the path gain of the  $l$ -th path associated with the  $m$ -th receive antenna. Since  $\mathbf{h}_m$  is not diagonal, ISI is generated. This can be remedied by using FDE.

The received signal block is transformed by an  $N_c$ -point fast Fourier transform (FFT) into the frequency-

domain signal,  $\mathbf{R}_m = [R_m(0), \dots, R_m(k), \dots, R_m(N_c - 1)]^T$ .  $\mathbf{R}_m$  is expressed as

$$\mathbf{R}_m = \mathbf{F} \mathbf{r}_m = \sqrt{\frac{2E_s}{T_s}} \mathbf{H}_m \mathbf{D} + \mathbf{N}_m, \quad (6)$$

where  $\mathbf{H}_m = \mathbf{F} \mathbf{h}_m \mathbf{F}^H$  is the channel matrix with  $\mathbf{F}$  being the FFT matrix of size  $N_c \times N_c$  and  $(\cdot)^H$  denoting the Hermitian transpose operation,  $\mathbf{D} = [D(0), \dots, D(k), \dots, D(N_c - 1)]^T = \mathbf{F} \mathbf{d}$  is the frequency-domain signal vector, and  $\mathbf{N}_m = [N_m(0), \dots, N_m(k), \dots, N_m(N_c - 1)]^T = \mathbf{F} \mathbf{n}_m$  is the frequency-domain noise vector.

Matrix  $\mathbf{H}_m = \mathbf{F} \mathbf{h}_m \mathbf{F}^H$  is diagonal because of the circulant property of  $\mathbf{h}_m$  and is given by

$$\mathbf{H}_m = \mathbf{F} \mathbf{h}_m \mathbf{F}^H = \begin{bmatrix} H_m(0) & & \mathbf{0} \\ & \ddots & \\ \mathbf{0} & & H_m(N_c - 1) \end{bmatrix}, \quad (7)$$

where  $H_m(k)$  is the channel gain at the  $k$ -th frequency. Since  $\mathbf{H}_m$  is diagonal, the  $k$ -th element,  $R_m(k)$ , of  $\mathbf{R}_m$  is given as

$$R_m(k) = \sqrt{\frac{2E_s}{T_s}} H_m(k) D(k) + N_m(k), \quad (8)$$

where  $H_m(k)$ ,  $D(k)$ , and  $N_m(k)$  are respectively given by

$$\begin{cases} H_m(k) = \sum_{l=0}^{L-1} h_{m,l} \exp\left(-j2\pi k \frac{\tau_l}{N_c}\right) \\ D(k) = \frac{1}{\sqrt{N_c}} \sum_{t=0}^{N_c-1} d(t) \exp\left(-j2\pi k \frac{t}{N_c}\right) \\ N_m(k) = \frac{1}{\sqrt{N_c}} \sum_{t=0}^{N_c-1} n_m(t) \exp\left(-j2\pi k \frac{t}{N_c}\right) \end{cases} \quad (9)$$

Using the one-tap FDE weight matrix of size  $N_c \times N_c$ ,  $\mathbf{W}_m = \text{diag}\{W_m(0), \dots, W_m(k), \dots, W_m(N_c - 1)\}$ , the frequency-domain received signal  $\hat{\mathbf{R}} = [\hat{R}(0), \dots, \hat{R}(k), \dots, \hat{R}(N_c - 1)]$  after joint FDE/antenna diversity combining can be expressed as

$$\hat{\mathbf{R}} = \sum_{m=0}^{N_r-1} \mathbf{W}_m \mathbf{R}_m = \sqrt{\frac{2E_s}{T_s}} \left( \sum_{m=0}^{N_r-1} \mathbf{W}_m \mathbf{H}_m \right) \mathbf{D} + \sum_{m=0}^{N_r-1} \mathbf{W}_m \mathbf{N}_m. \quad (10)$$

The  $k$ -th element of  $\hat{\mathbf{R}}$ ,  $\hat{R}(k)$ , is given as

$$\hat{R}(k) = \sum_{m=0}^{N_r-1} W_m(k) R_m(k) = \sqrt{\frac{2E_s}{T_s}} \hat{H}(k) D(k) + \hat{N}(k), \quad (11)$$

where  $\hat{H}(k)$  is called the equivalent channel gain and  $\hat{N}(k)$  is the noise after FDE, and each is defined as

$$\begin{cases} \hat{H}(k) = \sum_{m=0}^{N_r-1} W_m(k) H_m(k) \\ \hat{N}(k) = \sum_{m=0}^{N_r-1} W_m(k) N_m(k) \end{cases} \quad (12)$$

Various FDE criteria exist. Below are the well-known equalization weights:

$$W_m(k) = \begin{cases} \frac{H_m^*(k)}{\sum_{m'=0}^{N_r-1} |H_{m'}(k)|^2}, & \text{ZF} \\ H_m^*(k)/|H_m(k)|, & \text{EGC} \\ H_m^*(k), & \text{MRC} \\ \frac{H_m^*(k)}{\sum_{m'=0}^{N_r-1} |H_{m'}(k)|^2 + (E_s/N_0)^{-1}}, & \text{MMSE} \end{cases}, \quad (13)$$

where  $*$  denotes the complex conjugate operation.

The zero-forcing (ZF) weight removes the phase rotation and amplitude distortion induced by the channel frequency-selectivity. Therefore, the frequency-nonsselective channel is perfectly restored, i.e.,  $\hat{H}(k) = 1$  always (of course, this is the case only for the ideal channel estimation case), but the noise is enhanced at a frequency where the channel gain drops. The equal-gain combining (EGC) weight only removes the channel induced phase rotation. The maximal-ratio combining (MRC) weight can avoid the noise enhancement problem and maximizes the signal-to-noise ratio (SNR), but enhances the frequency-selectivity of the equivalent channel (i.e., the channel after equalization). The minimum mean square error (MMSE) weight minimizes the mean square of the equalization error,  $e(k)$ , defined as  $e(k) = \hat{R}(k) - D(k) = \sum_{m=0}^{N_r-1} W_m(k) R_m(k) - D(k)$  and therefore, can tradeoff the frequency-nonsselective channel restoration and the noise enhancement.

If  $\sum_{m=0}^{N_r-1} |H_m(k)|^2 \gg (E_s/N_0)^{-1}$ , the MMSE weight approximates the ZF weight. On the other hand, if  $\sum_{m=0}^{N_r-1} |H_m(k)|^2 \ll (E_s/N_0)^{-1}$ , the MMSE weight approaches  $(E_s/N_0) H_m^*(k)$  and approximates the MRC weight so that the noise enhancement problem is avoided and the SNR is maximized. In this way, the MMSE weight can best compromise between the restoration of the frequency-nonsselective channel and the noise enhancement.

Figure 3 shows a one shot observation of original propagation channel gain  $H_m(k)$ , FDE weight  $W_m(k)$ , equivalent channel gain  $\hat{H}(k)$ , and noise  $\hat{N}(k)$  for a symbol-spaced  $L = 16$ -path uniform power delay profile ( $E[|h_{m,l}|^2] = 1/L$  for all  $m$  and  $l$ ). As discussed above, it can be clearly seen for a no-antenna-diversity case ( $N_r = 1$ ) that the MMSE weight can avoid the noise enhancement by giving up the frequency-nonsselective channel restoration. However, for an antenna diversity case ( $N_r = 2$ ), the difference between ZF and MMSE weights diminishes.

The block of soft decision variables,  $\hat{\mathbf{d}} = [\hat{d}(0), \dots, \hat{d}(t), \dots, \hat{d}(N_c - 1)]^T$ , associated with the transmitted symbol block,  $\mathbf{d} = [d(0), \dots, d(t), \dots, d(N_c - 1)]^T$ , is obtained by applying an  $N_c$ -point inverse FFT (IFFT) to  $\hat{\mathbf{R}} = [\hat{R}(0), \dots, \hat{R}(k), \dots, \hat{R}(N_c - 1)]^T$  as

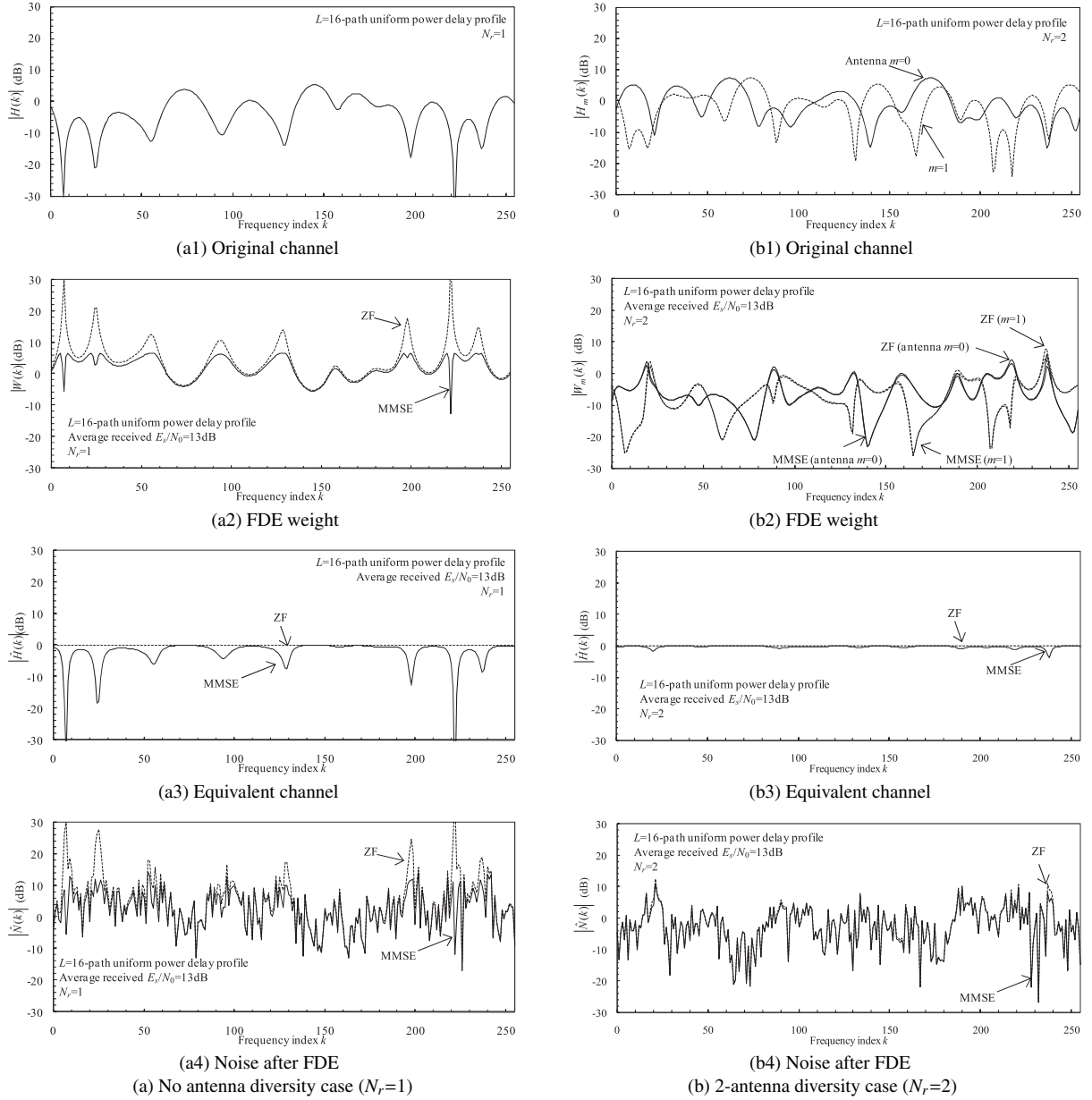


Fig. 3 One shot observation of  $H_m(k)$ ,  $W_m(k)$ ,  $\hat{H}(k)$ , and  $\hat{N}(k)$  for ZF- and MMSE-FDE.

$$\hat{\mathbf{d}} = \mathbf{F}^H \hat{\mathbf{R}} = \sqrt{\frac{2E_s}{T_s}} (\mathbf{F}^H \hat{\mathbf{H}} \mathbf{F}) \mathbf{d} + \mathbf{F}^H \hat{\mathbf{N}} \quad (14)$$

since  $\mathbf{D} = \mathbf{F} \mathbf{d}$ , where  $\hat{\mathbf{H}} = \text{diag} \{ \hat{H}(0), \dots, \hat{H}(k), \dots, \hat{H}(N_c - 1) \}$  and  $\hat{\mathbf{N}} = [\hat{N}(0), \dots, \hat{N}(k), \dots, \hat{N}(N_c - 1)]^T$  with

$$\begin{cases} \hat{\mathbf{H}} = \sum_{m=0}^{N_r-1} \mathbf{W}_m \mathbf{H}_m \\ \hat{\mathbf{N}} = \sum_{m=0}^{N_r-1} \mathbf{W}_m \mathbf{N}_m \end{cases} \quad (15)$$

From Eq. (14),  $\hat{d}(t)$  is given as

$$\hat{d}(t) = \sqrt{\frac{2E_s}{T_s}} \left( \frac{1}{N_c} \sum_{k=0}^{N_c-1} \hat{H}(k) \right) d(t)$$

$$\begin{aligned} & + \frac{1}{N_c} \sum_{k=0}^{N_c-1} \hat{H}(k) \left[ \sqrt{\frac{2E_s}{T_s}} \sum_{\substack{t'=0 \\ \neq t}}^{N_c-1} d(t') \exp \left( j2\pi k \frac{t-t'}{N_c} \right) \right] \\ & + \hat{n}(t), \end{aligned} \quad (16)$$

where the first term is a scaled version of the desired symbol,  $d(t)$ , to be detected, the second term is the residual ISI, and the third term is the noise resulting from  $\mathbf{F}^H \hat{\mathbf{N}}$ . Equation (16) shows that the channel gain associated with  $d(t)$  is the equivalent channel gain averaged over  $N_c$  frequencies, i.e.,  $(1/N_c) \sum_{k=0}^{N_c-1} \hat{H}(k)$ , and hence, the frequency diversity gain can be achieved. The use of MMSE-FDE significantly improves the BER performance. However, the presence of residual ISI after FDE (the second term of Eq. (16)) limits the performance improvement (introducing residual ISI can-

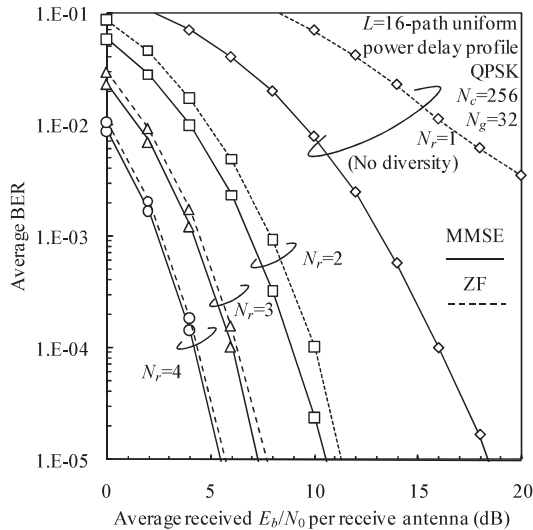


Fig. 4 BER performance of SC with FDE.

cellation can achieve a performance level that is very close to the theoretical lower bound [13]).

Figure 4 illustrates the achievable average BER performance of SC with MMSE-FDE and ZF-FDE with the number of receive antennas,  $N_r$ , as a parameter. Coherent quadrature phase shift keying (QPSK) data-modulation is used. The channel is assumed to be a frequency-selective block Rayleigh fading channel having an  $L = 16$ -path uniform power delay profile. MMSE-FDE provides better BER performance than ZF-FDE. However, it is interesting to note that as  $N_r$  increases, the performance gap between MMSE-FDE and ZF-FDE becomes narrower since  $\sum_{m=0}^{N_r-1} |H_m(k)|^2 \gg (E_s/N_0)^{-1}$  most of the time and the MMSE and ZF weights are almost the same.

### 3. Combining SC and FDMA

A big advantage of orthogonal frequency division multiple access (OFDMA) is its high level of robustness against frequency-selective fading [14] and the fact that it does not cause MAI at all if a different group of subcarriers is assigned to each user. However, the OFDMA waveform exhibits very profound amplitude fluctuations, resulting in a high PAPR. Therefore, very expensive linear power amplifiers that have a wide dynamic range are required. This is a problem when OFDMA is applied to the uplinks (mobile-to-base) in cellular communications systems.

SC transmission can be combined with FDMA (referred to as SC-FDMA or DFT-spread OFDMA) [15]–[20]. SC-FDMA is adopted as the uplink multiple access technique in 3G long-term evolution (LTE) systems [21]. The uplink transmitter/receiver structure of SC-FDMA is illustrated in Fig. 5. The transmit symbol block for each user is transformed into a frequency-domain signal by using the discrete Fourier transform (DFT). The frequency components for each user are mapped onto a different group of subcarriers so that they do not overlap each other in order

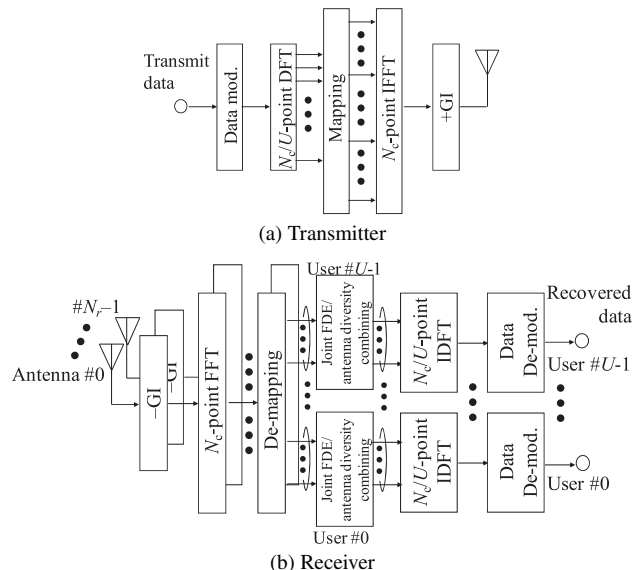


Fig. 5 Uplink transmitter/receiver structure of SC-FDMA.

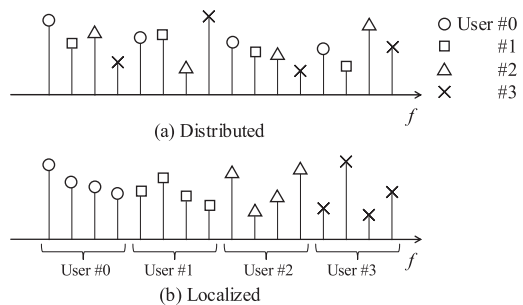


Fig. 6 Distributed and localized SC-FDMA when  $U = 4$ .

to eliminate the MAI. Then, the SC-FDMA signal is generated by applying the IFFT to the frequency-domain signal. If DFT is not used, the OFDMA signal is generated.

To retain the low PAPR property of SC-FDMA signals, subcarriers in each group are either equidistantly distributed or localized. In the distributed SC-FDMA (or the interleaved FDMA), the frequency components for each user are spread over the entire system bandwidth. The bandwidth of the localized SC-FDMA signal is a fraction of the system bandwidth. Figure 6 compares distributed and localized SC-FDMA when  $U = 4$ .

Let us consider the signal representation of distributed SC-FDMA using  $N_c$  subcarriers. Assuming that  $U$  users are simultaneously transmitting their signals, an equal number of subcarriers, i.e.,  $N_c/U$ , is assigned to each user, where  $N_c/U$  is an integer. The size of the transmit symbol block for each user is  $N_c/U$  symbols. The transmit symbol block for the  $u$ -th user,  $\mathbf{d}_u = [d_u(0), \dots, d_u(t), \dots, d_u(N_c/U - 1)]^T$ , is transformed into frequency-domain signal  $\mathbf{D}_u = [D_u(0), \dots, D_u(q), \dots, D_u(N_c/U - 1)]^T$  by using an  $N_c/U$ -point DFT as

$$\mathbf{D}_u = \mathbf{F}_{N_c/U} \mathbf{d}_u, \quad (17)$$

where  $\mathbf{F}_{N_c/U}$  is the DFT matrix of size  $N_c/U \times N_c/U$ . The  $q$ -th element of  $\mathbf{D}_u$  is given by

$$D_u(q) = \frac{1}{\sqrt{N_c/U}} \sum_{t=0}^{N_c/U-1} d_u(t) \exp\left(-j2\pi q \frac{t}{N_c/U}\right). \quad (18)$$

$N_c/U$  frequency components are equidistantly mapped over the entire system bandwidth consisting of  $N_c$  subcarriers. A group of subcarriers assigned to the  $u$ -th user is  $\{k = u + qU; q = 0 \sim (N_c/U - 1)\}$ . The SC-FDMA signal of the  $u$ -th user is given a frequency shift equivalent to  $u$  times the subcarrier separation,  $u/T$ , where  $T$  is the  $N_c$ -point FFT block length in time. The frequency-domain signal after mapping,  $\mathbf{X}_u = [X_u(0), \dots, X_u(k), \dots, X_u(N_c - 1)]^T$ , can be expressed as

$$\mathbf{X}_u = \mathbf{Q}_u \mathbf{D}_u, \quad (19)$$

where  $\mathbf{Q}_u$  is the mapping matrix of size  $N_c \times (N_c/U)$ . Below is an example of  $\mathbf{Q}_0$  and  $\mathbf{Q}_1$  for the case of  $N_c = 4$  and  $U = 2$ :

$$\mathbf{Q}_0 = \begin{bmatrix} 1 & 0 \\ 0 & 0 \\ 0 & 1 \\ 0 & 0 \end{bmatrix}, \mathbf{Q}_1 = \begin{bmatrix} 0 & 0 \\ 1 & 0 \\ 0 & 0 \\ 0 & 1 \end{bmatrix} \text{ for } N_c = 4 \text{ and } U = 2. \quad (20)$$

The SC-FDMA signal,  $\mathbf{x}_u = [x_u(0), \dots, x_u(t), \dots, x_u(N_c - 1)]^T$ , is generated using an  $N_c$ -point IFFT as (note that  $\mathbf{F}$  denotes the FFT matrix of size  $N_c \times N_c$ )

$$\mathbf{x}_u = \mathbf{F}^H \mathbf{X}_u = \mathbf{F}^H \mathbf{Q}_u \mathbf{D}_u. \quad (21)$$

It should be noted that the  $t$ -th element,  $x_u(t)$ , of  $\mathbf{x}_u$  is given by

$$\begin{aligned} x_u(t) &= \frac{1}{\sqrt{N_c}} \sum_{k=0}^{N_c-1} X_u(k) \exp\left(j2\pi t \frac{k}{N_c}\right) \\ &= \frac{1}{\sqrt{N_c}} \sum_{q=0}^{N_c/U-1} D_u(q) \exp\left(j2\pi t \frac{u+qU}{N_c}\right) \\ &= \frac{1}{\sqrt{U}} d_u(t \bmod (N_c/U)) \exp\left(j2\pi t \frac{u}{N_c}\right) \end{aligned} \quad (22)$$

and hence, the distributed SC-FDMA signal can also be generated first by time-compressing the  $N_c/U$ -symbol block,  $\mathbf{d}_u$ , by a factor of  $U$ , second by repeating it  $U$  times, and third by applying the user specific phase rotation (or frequency shift) [16]. This signal generation method does not require an  $N_c/U$ -point DFT and an  $N_c$ -point IFFT.

The idea of distributed SC-FDMA can be applied to SC-CDMA. One such application is the variable spreading and chip repetition factor CDMA (VSCRF-CDMA) [22]. Another application is the frequency-interleaved spread spectrum multiple access (FI-SSMA) [23]. FI-SSMA using equidistant subcarrier mapping is equivalent to VSCRF-CDMA.

We assume slow transmit power control (TPC) so that the average received signal power is kept the same for all

users. The GI-removed received signal block at the  $m$ -th receive antenna is a superposition of SC-FDMA signals transmitted from  $U$  users and can be expressed using the matrix form as

$$\mathbf{r}_m = \sqrt{\frac{2E_s}{T_s}} \sum_{u=0}^{U-1} \mathbf{h}_{u,m} \mathbf{x}_u + \mathbf{n}_m, \quad (23)$$

where  $\mathbf{h}_{u,m}$  is the  $u$ -th user's equivalent channel matrix of size  $N_c \times N_c$ , given by Eq. (5). The received signal block  $\mathbf{r}_m$  is transformed into frequency-domain signal,  $\mathbf{R}_m = [R_m(0), \dots, R_m(k), \dots, R_m(N_c - 1)]^T$ , by using an  $N_c$ -point FFT.  $\mathbf{R}_m$  can be expressed as

$$\mathbf{R}_m = \mathbf{F} \mathbf{r}_m = \sqrt{\frac{2E_s}{T_s}} \sum_{u=0}^{U-1} \mathbf{H}_{u,m} \mathbf{X}_u + \mathbf{N}_m, \quad (24)$$

where  $\mathbf{H}_{u,m} = \mathbf{F} \mathbf{h}_{u,m} \mathbf{F}^H = \text{diag}\{H_{u,m}(0), \dots, H_{u,m}(k), \dots, H_{u,m}(N_c - 1)\}$  and  $\mathbf{N}_m = [N_m(0), \dots, N_m(k), \dots, N_m(N_c - 1)]^T$  is the noise vector.

After performing an  $N_c$ -point FFT, subcarrier demapping is performed to extract the frequency-domain signal,  $\mathbf{R}_{u,m} = [R_{u,m}(0), \dots, R_{u,m}(q), \dots, R_{u,m}(N_c/U - 1)]^T$ , for the  $u$ -th user as

$$\mathbf{R}_{u,m} = \mathbf{Q}'_u \mathbf{R}_m. \quad (25)$$

Since

$$\mathbf{Q}'_u \mathbf{H}_{u',m} \mathbf{Q}'_u = \begin{cases} \tilde{\mathbf{H}}_{u,m} = \text{diag}\{\tilde{H}_{u,m}(0), \dots, \tilde{H}_{u,m}(q), \\ \dots, \tilde{H}_{u,m}(N_c/U - 1)\} & \text{if } u' = u \\ [0, \dots, 0, \dots, 0] & \text{otherwise} \end{cases} \quad (26)$$

with  $\tilde{H}_{u,m}(q) = H_{u,m}(k = u + qU)$ , Eq. (25) becomes

$$\mathbf{R}_{u,m} = \tilde{\mathbf{H}}_{u,m} \mathbf{D}_u + \mathbf{Q}'_u \mathbf{N}_m. \quad (27)$$

Joint FDE/antenna diversity combining is performed as

$$\begin{aligned} \hat{\mathbf{R}}_u &= [\hat{R}_u(0), \dots, \hat{R}_u(q), \dots, \hat{R}_u(N_c/U - 1)]^T \\ &= \sum_{m=0}^{N_r-1} \mathbf{W}_{u,m} \mathbf{R}_{u,m} = \sqrt{\frac{2E_s}{T_s}} \hat{\mathbf{H}}_u \mathbf{D}_u + \hat{\mathbf{N}}_u, \end{aligned} \quad (28)$$

where  $\hat{\mathbf{H}}_u = \text{diag}\{\hat{H}_u(0), \dots, \hat{H}_u(q), \dots, \hat{H}_u(N_c/U - 1)\}$ ,  $\hat{\mathbf{N}}_u = [\hat{N}_u(0), \dots, \hat{N}_u(q), \dots, \hat{N}_u(N_c/U - 1)]^T$ , and

$$\begin{cases} \hat{\mathbf{H}}_u = \sum_{m=0}^{N_r-1} \mathbf{W}_{u,m} \tilde{\mathbf{H}}_{u,m} \\ \hat{\mathbf{N}}_u = \sum_{m=0}^{N_r-1} \mathbf{W}_{u,m} \mathbf{Q}'_u \mathbf{N}_m \end{cases} \quad (29)$$

$\mathbf{W}_{u,m} = \text{diag}\{W_{u,m}(0), \dots, W_{u,m}(q), \dots, W_{u,m}(N_c/U - 1)\}$  is the one-tap MMSE weight matrix and its  $q$ -th element,  $W_{u,m}(q)$ , is given by

$$W_{u,m}(q) = \frac{\tilde{H}_{u,m}^*(q)}{\sum_{m'=0}^{N_r-1} |\tilde{H}_{u,m'}(q)|^2 + (E_s/N_0)^{-1}} \quad \text{for MMSE.} \quad (30)$$

The block of soft decision variables,  $\hat{\mathbf{d}}_u = [d_u(0), \dots, d_u(t), \dots, d_u(N_c/U - 1)]$ , is obtained by using an  $N_c/U$ -point inverse DFT (IDFT) as

$$\begin{aligned} \hat{\mathbf{d}}_u &= \mathbf{F}_{N_c/U}^H \hat{\mathbf{R}}_u \\ &= \sqrt{\frac{2E_s}{T_s}} (\mathbf{F}_{N_c/U}^H \hat{\mathbf{H}}_u \mathbf{F}_{N_c/U}) \mathbf{d}_u + \mathbf{F}_{N_c/U}^H \hat{\mathbf{N}}_u \end{aligned} \quad (31)$$

since  $\mathbf{D}_u = \mathbf{F}_{N_c/U} \mathbf{d}_u$ . A comparison of Eqs. (14) and (31) shows that SC-FDMA is equivalent to SC with FDE for transmitting a data symbol block of size  $N_c/U$  (however, note that the subcarrier separation in frequency is  $U$  times larger).

Figure 7 compares the uplink BER performance of distributed and localized SC-FDMA with MMSE-FDE for  $N_c = 256$ ,  $N_g = 32$ ,  $U = 16$ , and coherent QPSK data-modulation. Slow TPC is assumed so that the average received signal power is kept the same for all users. The distributed SC-FDMA provides better BER performance than the localized SC-FDMA. This is because the frequency-domain signal for each user is spread over the entire bandwidth, thereby achieving a higher frequency-diversity gain. On the other hand, in the localized SC-FDMA, since the frequency components for each user are mapped onto a group of adjacent subcarriers, they may experience almost the same fading and hence, the frequency diversity gain is lower than that in the distributed SC-FDMA.

However, it is worthwhile noting that the user scheduling can be introduced into the localized SC-FDMA to achieve the multi-user diversity gain by exploiting the fact that each user experiences a different fading channel. In a cellular system, the received signal power changes significantly due to shadowing and distance-dependent path loss in addition to fading and therefore, a large multi-user diversity gain can be achieved. A user who is experiencing better channel conditions is given higher priority transmission; this

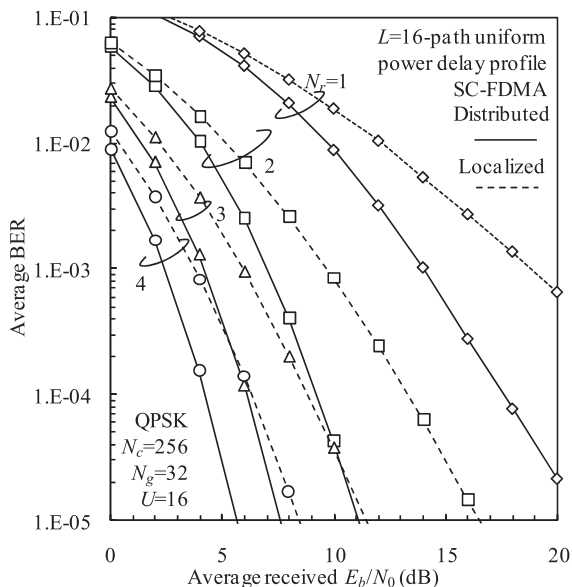


Fig. 7 Uplink BER performance of SC-FDMA.

tends to cause a fairness problem because users experiencing poor channel conditions cannot be given an opportunity to transmit their signal. However, this can be remedied by using scheduling methods taking into account the fairness problem [24], [25]. The localized SC-FDMA relies more on the multi-user diversity gain than the frequency diversity gain.

## 4. Introduction of FDE to SC-CDMA

### 4.1 Frequency-Domain Chip Equalization

The principle of SC with FDE was presented in Sect. 2. In this section, we extend the discussion to SC-CDMA. Figure 8 illustrates the transmitter/receiver structure for SC-CDMA.

The transmission of an  $N_c$ -chip block of multicode SC-CDMA with the spreading factor  $SF$  and the code multiplexing order  $U$  is considered.  $N_c/SF$  is assumed to be an integer. At the transmitter, data symbol block  $\{d(n); n = 0 \sim (U(N_c/SF) - 1)\}$  is serial-to-parallel (S/P) converted into  $U$  parallel streams,  $\{d_u(n'); n' = 0 \sim (N_c/SF - 1), u = 0 \sim U - 1, \text{ where } U/SF \leq 1\}$ . Then, each stream is spread using orthogonal spreading code  $\{c_u(t); t = 0 \sim SF - 1\}$  with  $|c_u(t)| = 1, u = 0 \sim U - 1$ , where  $SF$  is the spreading factor and variable  $t$  represents the chip-spaced discrete time. After multiplexing  $U$  chip streams and then multiplying scrambling code  $\{c_{scr}(t); t = 0 \sim (N_c - 1)\}$  with  $|c_{scr}(t)| = 1$ , the multicode SC-CDMA signal,  $s(t)$ , is generated.  $s(t)$  can be expressed as

$$s(t) = \sqrt{\frac{2E_c}{T_c}} \left[ \sum_{u=0}^{U-1} d \left( \left\lfloor \frac{t + uN_c}{SF} \right\rfloor \right) c_u(t \bmod SF) \right] c_{scr}(t), \quad (32)$$

where  $E_c (=E_s/SF)$  and  $T_c (=T_s/SF)$  are the chip energy per parallel stream and the chip duration, respectively, and  $\lfloor x \rfloor$  represents the largest integer smaller than or equal to  $x$ .

The multicode SC-CDMA signal,  $\{s(t); t = 0 \sim (N_c - 1)\}$ , can be expressed using the matrix form as

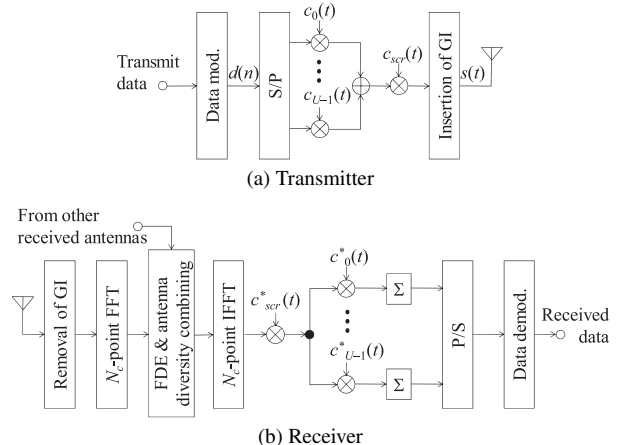


Fig. 8 Transmitter/receiver structure for SC-CDMA.

$$\mathbf{s} = [s(0), \dots, s(t), \dots, s(N_c - 1)]^T = \sqrt{\frac{2E_c}{T_c}} \mathbf{c} \mathbf{d}, \quad (33)$$

where  $\mathbf{d} = [d(0), \dots, d(n), \dots, d(U(N_c/SF) - 1)]^T$  is the data symbol vector and  $\mathbf{c}$  is the spreading matrix of size  $N_c \times U(N_c/SF)$ , given as

$$\mathbf{c} = \mathbf{c}_{scr} \cdot \begin{bmatrix} \mathbf{c}_0 & \mathbf{0} & \mathbf{c}_1 & \mathbf{0} & \dots & \mathbf{c}_{U-1} & \mathbf{0} \\ \vdots & \ddots & \vdots & \ddots & \ddots & \vdots & \ddots \\ \mathbf{0} & \mathbf{c}_0 & \mathbf{0} & \mathbf{c}_1 & \mathbf{0} & \dots & \mathbf{c}_{U-1} \end{bmatrix} \quad (34)$$

with  $\mathbf{c}_u = [c_u(0), \dots, c_u(t), \dots, c_u(SF - 1)]^T$  and  $\mathbf{c}_{scr} = \text{diag} \{c_{scr}(0), \dots, c_{scr}(t), \dots, c_{scr}(N_c - 1)\}$ . Substituting Eq. (32) into Eq. (4), the GI-removed received signal,  $\mathbf{r}_m = [r_m(0), \dots, r_m(t), \dots, r_m(N_c - 1)]^T$ , at the  $m$ -th receive antenna can be expressed as

$$\mathbf{r}_m = \sqrt{\frac{2E_c}{T_c}} (\mathbf{h}_m \mathbf{c}) \mathbf{d} + \mathbf{n}_m, \quad (35)$$

where  $\mathbf{h}_m$  is the channel matrix of size  $N_c \times N_c$ , given by Eq. (5), and  $\mathbf{n}_m$  is the noise vector of size  $N_c \times 1$ .

The received signal,  $\mathbf{r}_m$ , is transformed by an  $N_c$ -point FFT into the frequency-domain signal,  $\mathbf{R}_m = [R_m(0), \dots, R_m(k), \dots, R_m(N_c - 1)]^T$ . Similar to Eq. (6),  $\mathbf{R}_m$  can be expressed as

$$\begin{aligned} \mathbf{R}_m &= \mathbf{F} \mathbf{r}_m = \sqrt{\frac{2E_c}{T_c}} (\mathbf{F} \mathbf{h}_m \mathbf{F}^H) (\mathbf{F} \mathbf{c}) \mathbf{d} + \mathbf{F} \mathbf{n}_m \\ &= \sqrt{\frac{2E_c}{T_c}} (\mathbf{H}_m \mathbf{C}) \mathbf{d} + \mathbf{N}_m, \end{aligned} \quad (36)$$

where  $\mathbf{C} = \mathbf{F} \mathbf{c}$  is the frequency-domain representation of spreading matrix  $\mathbf{c}$  (note that  $\mathbf{F}$  is the FFT matrix of size  $N_c \times N_c$ ). The frequency-domain received signal,  $\hat{\mathbf{R}}$ , after joint FDE/antenna diversity combining can be expressed as

$$\hat{\mathbf{R}} = \sum_{m=0}^{N_r-1} \mathbf{W}_m \mathbf{R}_m = \sqrt{\frac{2E_c}{T_c}} (\hat{\mathbf{H}} \mathbf{C}) \mathbf{d} + \hat{\mathbf{N}}, \quad (37)$$

where  $\hat{\mathbf{H}}$  and  $\hat{\mathbf{N}}$  are defined by Eq. (15) and the  $k$ -th element,  $W_m(k)$ , of  $\mathbf{W}_m$  is given by Eq. (11) by replacing  $E_s/N_0$  with  $(U/SF)(E_s/N_0)$ .

After applying an  $N_c$ -point IFFT to  $\hat{\mathbf{R}} = [\hat{R}(0), \dots, \hat{R}(k), \dots, \hat{R}(N_c - 1)]^T$ , despreading is performed on the IFFT output signal block to obtain the decision variable block,  $\hat{\mathbf{d}} = [\hat{d}(0), \dots, \hat{d}(n), \dots, \hat{d}(U(N_c/SF) - 1)]^T$ , as

$$\hat{\mathbf{d}} = \frac{1}{SF} \mathbf{c}^H (\mathbf{F}^H \hat{\mathbf{R}}) = \sqrt{\frac{2E_c}{T_c}} \left( \frac{1}{SF} \mathbf{c}^H \hat{\mathbf{H}} \mathbf{C} \right) \mathbf{d} + \frac{1}{SF} \mathbf{c}^H \hat{\mathbf{N}} \quad (38)$$

since  $\mathbf{c}^H \mathbf{F}^H = (\mathbf{F} \mathbf{c})^H = \mathbf{C}^H$ . Note that if  $\mathbf{c} = \mathbf{I}$  (i.e.,  $SF = U = 1$ ), then  $\mathbf{C} = \mathbf{F}$  and as a consequence, Eq. (38) reduces to the non-spread SC case of Eq. (14). Therefore, it can be understood that  $\mathbf{C}$  has the same role as  $\mathbf{F}$  to spread the symbol energy to the entire signal bandwidth.

From Eq. (38), the expression for decision variable,  $\hat{d}(n)$ , associated with  $d(n)$  can be obtained as

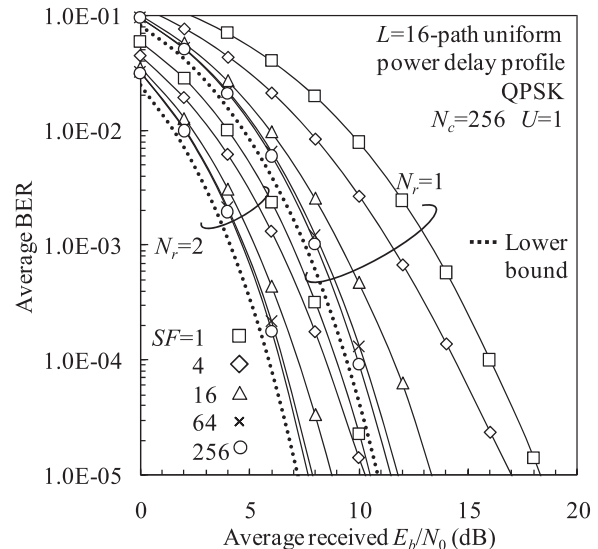


Fig. 9 Average BER performance of single-code SC-CDMA ( $U = 1$ ).

$$\begin{aligned} \hat{d}(n) &= \sqrt{\frac{2E_c}{T_c}} \left( \frac{1}{N_c} \sum_{k=0}^{N_c-1} \hat{H}(k) \right) d(n) \\ &+ \frac{1}{SF} \sum_{t=n'SF}^{(n'+1)SF} c^*(t, n) \left[ \frac{1}{N_c} \sum_{k=0}^{N_c-1} \hat{H}(k) \left\{ \sum_{\substack{t'=0 \\ \neq t}}^{N_c-1} s(t') \exp \left( j2\pi k \frac{t-t'}{N_c} \right) \right\} \right] \\ &+ \frac{1}{SF} \sum_{t=n'SF}^{(n'+1)SF} c^*(t, n) \left[ \frac{1}{N_c} \sum_{k=0}^{N_c-1} \hat{N}(k) \exp \left( j2\pi k \frac{t}{N_c} \right) \right], \end{aligned} \quad (39)$$

where  $n' = n \bmod (N_c/SF)$  and  $\{c(t, n); t = 0 \sim (N_c - 1)\}$  is the spreading code (which is the  $n$ -th column vector of  $\mathbf{c}$  and has  $SF$  nonzero elements and  $(N_c - SF)$  zero's) used for spreading the  $n$ -th data symbol. The first term is a scaled version of the desired symbol to be detected, the second term is the inter-code interference resulting from the residual ICI, and the third term is the noise. Similar to the non-spread SC case, the channel gain in the time-domain signal representation is  $(1/N_c) \sum_{k=0}^{N_c-1} \hat{H}(k)$  and hence, the high frequency diversity gain can be achieved irrespective of  $SF$ . The presence of residual ICI limits the performance improvement. The residual ICI can be suppressed more by increasing the value of  $SF$  (or at the cost of lowering the data rate) for the given  $E_s/N_0$ .

The average BER performance of single-code ( $U = 1$ ) SC-CDMA using MMSE-FDE in a frequency-selective block Rayleigh fading channel having an  $L = 16$ -path uniform power delay profile is plotted with  $SF$  as a parameter in Fig. 9 for  $N_c = 256$  and coherent QPSK data-modulation. Also plotted is the theoretical lower bound performance [26]. As  $SF$  increases, the performance improves due to better suppression of the residual ICI. Figure 10 plots the average BER performance of multi-code SC-CDMA ( $U > 1$ ). Again, MMSE-FDE is assumed. As  $U$  increases, the BER performance gradually degrades due to the increasing residual ICI.

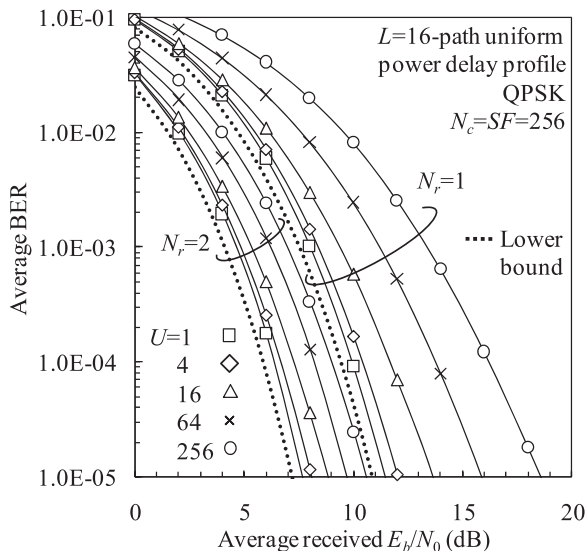


Fig. 10 Average BER performance of multi-code SC-CDMA ( $U > 1$ ).

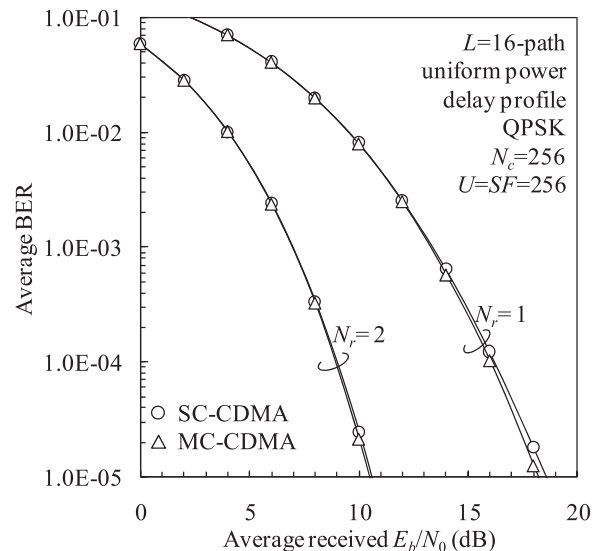


Fig. 12 Performance comparison between SC-CDMA and MC-CDMA for full-code multiplexing.

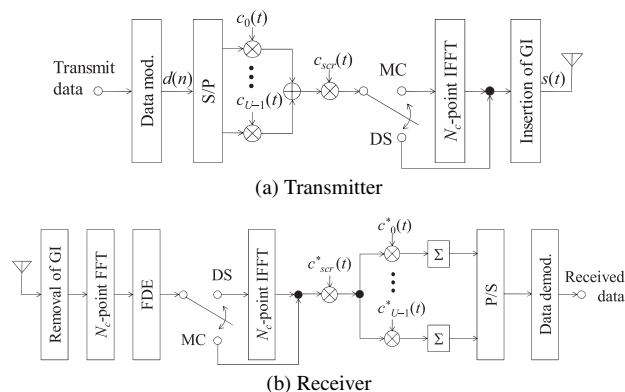


Fig. 11 Transmitter/receiver structure for SC- and MC-CDMA.

#### 4.2 Similarity of SC- and MC-CDMA

The similarities in the transmitter/receiver structure for SC-CDMA compared to MC-CDMA are shown in Fig. 11. For MC-CDMA, an  $N_c$ -point IFFT is applied at the transmitter to generate the time-domain MC-CDMA signal with  $N_c$  sub-carriers. In SC-CDMA, however, no IFFT is required. At the receiver, the received signal block is transformed by an  $N_c$ -point FFT into the frequency-domain signal of  $N_c$  sub-carriers to perform FDE. For SC-CDMA, the time-domain chip sequence is recovered by applying an  $N_c$ -point IFFT to the frequency-domain received signal after FDE, while it is not required for MC-CDMA.

As a consequence, the difference between SC-CDMA and MC-CDMA is only the location of the IFFT function as shown in Fig. 11. The IFFT is required at the transmitter for MC, while it is required at the receiver for SC. This allows a flexible transceiver design, which can switch between SC-CDMA and MC-CDMA, based on software-defined radio technology.

The signal representations for SC-CDMA with joint FDE/antenna diversity combining are given in Eqs. (32)–(38). For MC-CDMA, the spreading matrix,  $\mathbf{c}$ , in Eq. (34) is replaced by  $\mathbf{F}^H \mathbf{c}$  and hence,  $\mathbf{r}_m$  is given as

$$\mathbf{r}_m = \sqrt{\frac{2E_c}{T_c}} \mathbf{h}_m (\mathbf{F}^H \mathbf{c}) \mathbf{d} + \mathbf{n}_m \quad \text{for MC-CDMA.} \quad (40)$$

Therefore, the frequency-domain signal,  $\mathbf{R}_m$ , is given as

$$\mathbf{R}_m = \mathbf{F} \mathbf{r}_m = \sqrt{\frac{2E_c}{T_c}} (\mathbf{H}_m \mathbf{c}) \mathbf{d} + \mathbf{N}_m \quad \text{for MC-CDMA.} \quad (41)$$

Joint FDE/antenna diversity combining is performed as

$$\hat{\mathbf{R}} = \sum_{m=0}^{N_r-1} \mathbf{W}_m \mathbf{R}_m = \sqrt{\frac{2E_c}{T_c}} (\hat{\mathbf{H}} \mathbf{c}) \mathbf{d} + \hat{\mathbf{N}} \quad \text{for MC-CDMA} \quad (42)$$

with

$$\begin{cases} \hat{\mathbf{H}} = \sum_{m=0}^{N_r-1} \mathbf{W}_m \mathbf{H}_m \\ \hat{\mathbf{N}} = \sum_{m=0}^{N_r-1} \mathbf{W}_m \mathbf{N}_m \end{cases}, \quad (43)$$

where  $\mathbf{W}_m$  is the joint FDE/antenna diversity combining weight matrix and is the same as SC-CDMA. The decision variable block,  $\hat{\mathbf{d}}$ , obtained by de-spreading is given as

$$\hat{\mathbf{d}} = \frac{1}{SF} \mathbf{c}^H \hat{\mathbf{R}} = \sqrt{\frac{2E_c}{T_c}} (\mathbf{c}^H \hat{\mathbf{H}} \mathbf{c}) \mathbf{d} + \frac{1}{SF} \mathbf{c}^H \hat{\mathbf{N}}$$

for MC-CDMA. (44)

If  $\mathbf{c} = \mathbf{I}$  (i.e.,  $SF = U = 1$ ), Eq. (44) reduces to the OFDM case.

It is worthwhile noting that  $\mathbf{c}$  in MC-CDMA plays an

equivalent role to  $\mathbf{C} = \mathbf{F}\mathbf{c}$  in SC-CDMA (compare Eqs. (38) and (44)). In SC-CDMA, each data-modulated symbol is spread over all  $N_c$  subcarriers due to  $\mathbf{C} = \mathbf{F}\mathbf{c}$ , while in MC-CDMA, it is spread over only  $SF$  subcarriers due to  $\mathbf{c}$ . If  $SF$  is smaller than  $N_c$ , the frequency diversity gain that can be achieved in MC-CDMA is smaller than in SC-CDMA. (Note that MC-CDMA introduced in Ref. [2] uses the spreading factor of  $SF = N_c$ . But, here we assume a general case of  $SF$  being smaller than or equal to  $N_c$ .) However, if code multiplexing is used, the BER performance is limited by the residual ICI and therefore, MC-CDMA achieves almost identical BER performance as SC-CDMA irrespective of the value of  $SF$ .

A performance comparison between SC-CDMA and MC-CDMA is shown in Fig. 12 for full-code multiplexing ( $U/SF = 1$  and  $SF = N_c = 256$ ). Walsh-Hadamard (WH) sequences are used as the spreading codes. It can be clearly seen that both types of CDMA provide almost identical BER performance.

## 5. Block Spreading to Achieve MAI-Free SC-CDMA

As discussed earlier, MMSE-FDE can be applied to SC-CDMA to replace coherent rake combining with a significantly improved BER performance. This is true for the downlink (base-to-mobile) case. However, in the uplink (mobile-to-base) case, different users' signals pass through different channels and the orthogonality among them is distorted severely. The resulting MAI limits the uplink BER performance with MMSE-FDE.

Removing the MAI can increase the link capacity of cellular CDMA systems with single frequency reuse (the same carrier frequency is reused at every base station). Multiuser detection (MUD) can suppress the uplink MAI [27]; however, its computational complexity grows exponentially with the number of users. Block spreading can be used to convert the MUD problem into a set of equivalent single-user equalization problems [28], [29]. The uplink capacity (defined as the maximum number of users accommodated) of a cellular CDMA system can be roughly given as [30]

$$\frac{U}{SF} = \frac{1}{(E_b/\eta_0)_{req}} \frac{1}{1+F}, \quad (45)$$

where  $(E_b/\eta_0)_{req}$  is the required signal-to-noise plus MAI power spectrum density ratio and  $F$  is the other-cell MAI-to-own cell MAI ratio. The value of  $F$  is approximately 0.7 [31] when the path loss exponent is 3.8 and the shadowing loss standard deviation is 8 dB. If the own-cell MAI can be perfectly removed, we have  $1+F \rightarrow F$  in the denominator of Eq. (45) and thus, the link capacity increases by approximately 2.3 times. Furthermore, if block spreading is applied to the downlink, user-independent downlink transmit power control can be introduced while allowing single frequency reuse. This contributes to increasing the downlink capacity.

The block spreading relies on the assumption that the channel is time-nonselective and the channel does not change during the transmission. If a mobile terminal travels

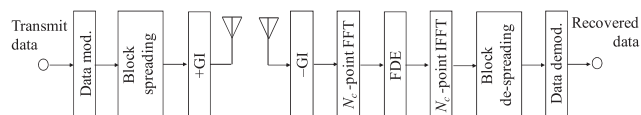


Fig. 13 Block spread SC-CDMA.

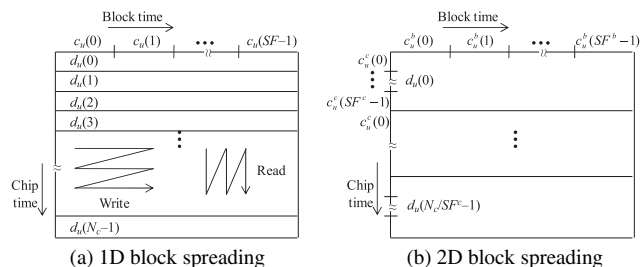


Fig. 14 Block spreading.

at a very high speed, the channel changes block-by-block and therefore, the orthogonal property among users is distorted and the MAI appears. Below, we assume a quasi-static channel so that the channel stays almost unchanged. Also assumed is ideal transmit timing control (i.e., the sum of the maximum time delay difference among the channels and the maximum transmit timing offset among users is kept shorter than the GI length).

### 5.1 One-Dimensional (1D) Spreading

For the sake of simplicity, we assume the same spreading factor,  $SF$ , for all users. The transmitter/receiver structure for block spread SC-CDMA is illustrated in Fig. 13. One-dimensional (1D) block spread SC-CDMA was presented in [28] and [29]. Below, we consider the transmission of a block of  $N_c$  data-modulated symbols. The chip sequence is written into a chip interleaver of size  $N_c \times SF$  row-by-row and is read out column-by-column, as shown in Fig. 14(a). Each column makes one  $N_c$ -chip block to be transmitted after insertion of the cyclic prefix (CP) into the guard interval (GI). In this way, the  $u$ -th user data block consisting of  $N_c$  data-modulated symbols,  $\mathbf{d}_u = [d_u(0), \dots, d_u(n), \dots, d_u(N_c - 1)]^T$ , is block spread by using spreading code  $\mathbf{c}_u = [c_u(0), \dots, c_u(q), \dots, c_u(SF - 1)]^T$ .

The 1D block spreading can be represented as an  $N_c \times SF$  matrix  $\tilde{\mathbf{x}}_u$  as

$$\tilde{\mathbf{x}}_u = [\mathbf{x}_u(0), \dots, \mathbf{x}_u(q), \dots, \mathbf{x}_u(SF - 1)] = \mathbf{d}_u \mathbf{c}_u^T, \quad (46)$$

where  $\mathbf{x}_u(q)$  is the  $q$ -th column vector of size  $N_c \times 1$ , representing the  $q$ -th chip block, as

$$\mathbf{x}_u(q) = \mathbf{d}_u \mathbf{c}_u(q) = [d_u(0), \dots, d_u(n), \dots, d_u(N_c - 1)]^T \mathbf{c}_u(q). \quad (47)$$

A sequence of  $N_c$ -chip blocks is transmitted over  $SF$  block periods after the insertion of an  $N_g$ -chip CP into the GI of each chip block.

The superposition of  $U$  users' signals that have passed

through different frequency-selective channels is received by the base station antenna. We assume ideal slow TPC so that the received signal power is kept the same for all users. Since we are assuming that the channel stays unchanged over a period of  $SF$  chip blocks, the  $N_c \times N_c$  channel matrix,  $\mathbf{h}_u(q)$ , of the  $u$ -th user at the  $q$ -th block time, given by Eq. (5), is  $\mathbf{h}_u(q) = \mathbf{h}_u$  for  $q = 0 \sim (SF - 1)$ . The GI-removed received signal can be represented by an  $N_c \times SF$  matrix,  $\mathbf{r}_{N_c \times SF}$ , as

$$\mathbf{r}_{N_c \times SF} = \sqrt{\frac{2E_c}{T_c}} \sum_{u=0}^{U-1} \mathbf{h}_u \tilde{\mathbf{x}}_u + \mathbf{n}_{N_c \times SF}, \quad (48)$$

where  $\mathbf{n}_{N_c \times SF}$  is an  $N_c \times SF$  noise matrix with each element having zero-mean and variance  $2N_0/T_c$  ( $N_0$  is the AWGN one-sided power spectrum density). Because of the CP insertion,  $\mathbf{h}_u$  is a circulant matrix with the first column given as  $[h_{u,0}, \dots, h_{u,l}, \dots, h_{u,L-1}, 0, \dots, 0]^T$ , where  $h_{u,l}$  is the  $l$ -th path gain of the  $u$ -th user channel.

Matrix  $\mathbf{r}_{N_c \times SF}$  is block-despread row-by-row using  $\mathbf{c}_u$  to obtain the block-despread signal  $\tilde{\mathbf{r}}_u$  of size  $N_c \times 1$ . Since  $(1/SF)\mathbf{c}_u^T \mathbf{c}_u^* = 1$ ,  $\tilde{\mathbf{r}}_u$  can be expressed as

$$\begin{aligned} \tilde{\mathbf{r}}_u &= \frac{1}{SF} \mathbf{r}_{N_c \times SF} \mathbf{c}_u^* \\ &= \sqrt{\frac{2E_c}{T_c}} \mathbf{h}_u \mathbf{d}_u + \sum_{\substack{u'=0 \\ u' \neq u}}^{U-1} \sqrt{\frac{2E_c}{T_c}} \tilde{\mathbf{h}}_{u'} \mathbf{d}_{u'} + \tilde{\mathbf{n}}_u \end{aligned} \quad (49)$$

with

$$\begin{cases} \tilde{\mathbf{h}}_{u'} = \left( \frac{1}{SF} \mathbf{c}_{u'}^T \mathbf{c}_u^* \right) \mathbf{h}_{u'} \\ \tilde{\mathbf{n}}_u = \frac{1}{SF} \mathbf{n}_{N_c \times SF} \mathbf{c}_u^* \end{cases}, \quad (50)$$

where  $\tilde{\mathbf{n}}_u$  is the noise vector of size  $N_c \times 1$ , whose elements are independent zero-mean complex Gaussian variables with variance  $(2N_0/T_c)/SF$ . In Eq. (49), the 1st and 2nd terms are respectively the desired signal component and the MAI component.

Assuming the orthogonal spreading codes,  $\mathbf{c}_{u'}^T \mathbf{c}_u^* = 0$  if  $u' \neq u$  and hence,  $\tilde{\mathbf{h}}_{u'} = \mathbf{0}$ . As a consequence, the MAI disappears. Since  $E_s = SF \cdot E_c$  and  $T_s = SF \cdot T_c$ , we have

$$\tilde{\mathbf{r}}_u = \sqrt{\frac{2E_s}{T_s}} \mathbf{h}_u \mathbf{d}_u + \tilde{\mathbf{n}}_u. \quad (51)$$

As many as  $U = SF$  users can be accommodated MAI-free. Equation (51) is identical to Eq. (4), which represents the non-spread SC signal received via a frequency-selective channel. Therefore, the single-user FDE, introduced in Sect. 2, can be applied to take advantage of the channel frequency-selectivity to improve the BER performance.

So far, a quasi-static fading environment has been assumed. However, if the channel varies in time (i.e., time-selective channel),  $\mathbf{h}_u(q) \neq \mathbf{h}_u$  for  $q = 0 \sim (SF - 1)$ . Hence,

$\tilde{\mathbf{h}}_{u'} \neq \mathbf{0}$  and the MAI appears. An interference cancellation technique must be used to reduce the MAI in a time-selective channel.

## 5.2 Two-Dimensional (2D) Spreading

1D block spread SC-CDMA uses the block spreading to achieve MAI-free multiple access while obtaining the frequency diversity gain. The spreading factor is used to remove the MAI only and cannot suppress the residual ISI resulting from the channel frequency-selectivity. Two-dimensional (2D) block spreading proposed in [32] can suppress the residual ISI and the other-cell interference while removing the MAI in a cellular SC-CDMA system.

As shown in Fig. 14(b), each data symbol to be transmitted is spread in both the chip-time and block time-domains using the 2D block spreading code, which is a product code of two orthogonal spreading codes. The spreading factor,  $SF$ , for the 2D block spreading is given by  $SF = SF^c \times SF^b$ , where  $SF^c$  and  $SF^b$  are the chip time-domain and block time-domain spreading factors, respectively. The 2D block spreading code for the  $u$ -th user can be represented using the matrix form as

$$\mathbf{c}_u = \mathbf{c}_u^c (\mathbf{c}_u^b)^T, \quad (52)$$

where  $\mathbf{c}_u$  is the matrix of size  $SF^c \times SF^b$  and  $\mathbf{c}_u^c = [c_u^c(0), \dots, c_u^c(t), \dots, c_u^c(SF^c - 1)]^T$  and  $\mathbf{c}_u^b = [c_u^b(0), \dots, c_u^b(t), \dots, c_u^b(SF^b - 1)]^T$  are the column vectors representing chip time-domain and block time-domain spreading codes, respectively. The block time-domain spreading is used to remove the MAI as 1D block spread SC-CDMA; up to  $U = SF^b$  users can be accommodated MAI-free. On the other hand, the chip time-domain spreading is used to suppress the residual ISI and the other-cell interference. If  $SF^c = 1$ , 2D block spread SC-CDMA reduces to 1D block spread SC-CDMA.

After block-despreading to remove the MAI, the  $N_c \times 1$  received signal,  $\tilde{\mathbf{r}}_u$ , can be expressed as

$$\tilde{\mathbf{r}}_u = \frac{1}{SF} \mathbf{r}_{N_c \times SF^b} (\mathbf{c}_u^b)^* = \sqrt{\frac{2E_s}{T_s}} (\mathbf{h}_u \tilde{\mathbf{c}}_u^c) \mathbf{d}_u + \tilde{\mathbf{n}}_u, \quad (53)$$

where  $\tilde{\mathbf{c}}_u^c = \text{diag}\{\mathbf{c}_u^c, \mathbf{c}_u^c, \dots, \mathbf{c}_u^c\}$  of size  $N_c \times N_c/SF^b$ ,  $\mathbf{d}_u = [d_u(0), \dots, d_u(n), \dots, d_u(N_c/SF^c)]^T$ , and  $\tilde{\mathbf{n}}_u = (1/SF) \mathbf{n}_{N_c \times SF^b} (\mathbf{c}_u^b)^*$ . A comparison of Eq. (53) and Eq. (35) confirms that  $\tilde{\mathbf{r}}_u$  is identical to the received SC-CDMA signal by replacing  $SF$  with  $SF^c$ . Since  $\mathbf{h}_u$  is not diagonal (see Eq. (5)), the ISI appears in  $\tilde{\mathbf{r}}_u$ . To eliminate the ISI and to improve the transmission performance, one-tap FDE can be applied in a similar manner to SC-CDMA (see Sect. 4). After transforming  $\tilde{\mathbf{r}}_u$  into a frequency-domain signal by using an  $N_c$ -point FFT, MMSE-FDE can be applied to improve the BER performance.

For a given  $SF$ , the block time-domain spreading factor  $SF^b$  should be as small as possible so that the chip time-domain spreading factor,  $SF^c$ , can be maximized to better reduce the residual ISI and the other-cell interference

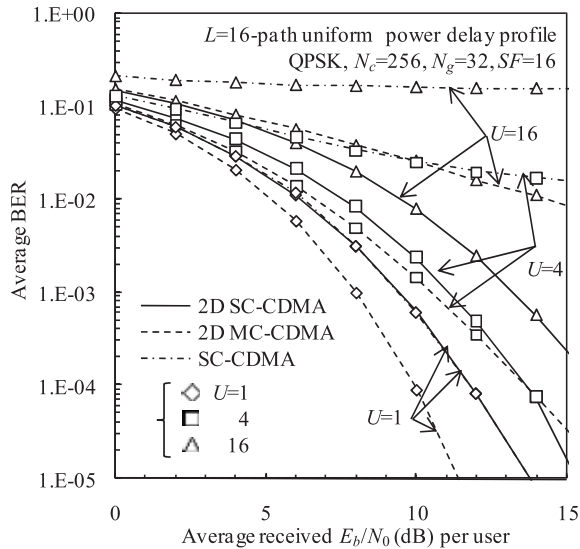


Fig. 15 Uplink BER performance of 2D block spread CDMA.

after MMSE-FDE. The optimum choice of  $(SF^c, SF^b)$  for the given total spreading factor  $SF$  is  $(SF/U, U)$ , where  $U$  should be a power of two.

The idea of block spreading can also be applied to MC-CDMA by replacing the chip time-domain spreading with the frequency-domain spreading (IFFT is necessary at the transmitter), resulting in MC DS-CDMA (called orthogonal multicarrier DS-CDMA-II in [33]).

Figure 15 plots the uplink BER performance of 2D block spread CDMA (2D SC-CDMA and 2D MC-CDMA in the figure) with  $(SF^c, SF^b) = (SF/U, U)$  and  $SF = 16$ . Ideal slow TPC and ideal transmit timing control are assumed. The BER performance of SC-CDMA is also plotted. When  $U = 1$ , 2D block spread SC- and MC-CDMA reduces to SC- and MC-CDMA, respectively. In this case, MC-CDMA provides better BER performance than SC-CDMA since no residual ISI is present in MC-CDMA while it is present in SC-CDMA. As  $U$  increases, the BER performance degrades. This is because the frequency diversity gain decreases due to reduced spreading factor  $SF^c$  in the chip-domain for the given total spreading factor  $SF = SF^c \times SF^b = 16$ . However, 2D block spread SC- and MC-CDMA provide significantly better BER performance than SC-CDMA.

In the above, the same  $SF$ , i.e., the same data rate, was assumed for all users. However, multi-rate transmission is possible even using the 1D and 2D block spreading by using the orthogonal variable spreading factor (OVSF) codes [34].

## 6. Utilization of Delay Time-Domain for Multiple Access

SC-FDMA separates users in the frequency domain, while block spread CDMA separates users in the spreading code domain. Another possible domain to separate users is the delay time-domain. A hybrid multiple access technique, called delay-time/CDMA (DT/CDMA), proposed in [35],

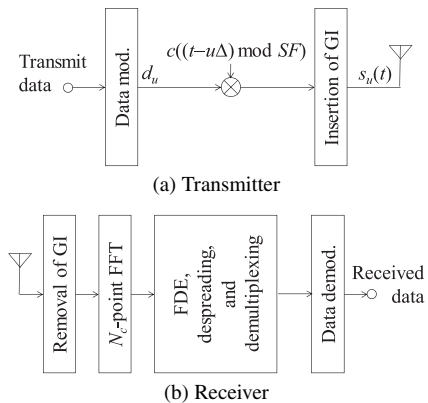


Fig. 16 Transmitter/receiver structure for DT/CDMA.

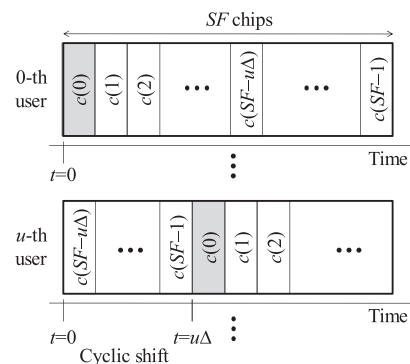


Fig. 17 Spreading codes for DT/CDMA.

suppresses the MAI while taking advantage of the channel frequency-selectivity to improve the BER performance. The idea of delay time-domain multiplexing can also be found in Ref. [36]. However, unlike the cyclic extended spread coded MC-CDMA proposed in Ref. [36], DT/CDMA performs the despreading, demultiplexing, and equalization simultaneously all in the frequency-domain.

The transmitter/receiver structure of DT/CDMA is illustrated in Fig. 16. DT/CDMA is a block transmission of  $SF$  chips, where  $SF$  is the spreading factor. A partial sequence of an  $SF$ -chip length taken from a long pseudo noise (PN) sequence  $\{c(t); t = nSF \sim (n+1)SF - 1\}$ , is shared by  $U$  users to spread their  $n$ -th data-modulated symbols.

A unique feature of DT/CDMA is that the  $u$ -th user ( $u = 0 \sim U - 1$ ) is assigned a cyclic time shift of  $u\Delta$  chips to its spreading code, where  $\Delta$  is longer than or equal to the maximum time delay difference of the channel in order to separate different users in the delay-time domain. The number of users that can be accommodated MAI-free is  $SF/\Delta$ . Below, we consider the case of  $U \leq SF/\Delta$  unless otherwise stated.

Without loss of generality, we consider the transmission of the  $n = 0$ -th symbol and drop the symbol index  $n$  for simplicity. The  $u$ -th user's data-modulated symbol,

$d_u$ , is spread by  $c((t - u\Delta) \bmod SF)$ ,  $t = 0 \sim SF - 1$ , as shown in Fig. 17. The  $u$ -th user's spread signal block,  $\mathbf{s}_u = [s_u(0), \dots, s_u(t), \dots, s_u(SF - 1)]^T$ , to be transmitted after inserting the CP into the GI can be expressed using the matrix form as

$$\mathbf{s}_u = \sqrt{\frac{2E_{c,u}}{T_c}} \mathbf{c}_u d_u, \quad (54)$$

where  $E_{c,u}$  represents the average transmit chip energy,

$$\mathbf{c}_u = \begin{bmatrix} c((0 - u\Delta) \bmod SF) \\ \vdots \\ c((t - u\Delta) \bmod SF) \\ \vdots \\ c((SF - 1 - u\Delta) \bmod SF) \end{bmatrix}, \quad (55)$$

and  $E[d_u^2] = 1$ .

A superposition of  $U$  users' signals is received at the base station. The GI-removed received signal block,  $\mathbf{r} = [r(0), \dots, r(t), \dots, r(SF - 1)]^T$ , can be expressed as

$$\mathbf{r} = \sum_{u=0}^{U-1} \sqrt{\frac{2E_{c,u}}{T_c}} \mathbf{h}_u \mathbf{c}_u d_u + \mathbf{n}, \quad (56)$$

where  $\mathbf{h}_u$  is the channel matrix of size  $SF \times SF$  and  $\mathbf{n}$  is the noise vector of size  $SF \times 1$ . The received signal block  $\mathbf{r}$  is transformed by using an  $SF$ -point FFT into the frequency-domain signal,  $\mathbf{R} = [R(0), \dots, R(k), \dots, R(SF - 1)]^T$ , as

$$\mathbf{R} = \mathbf{F}\mathbf{r} = \sum_{u=0}^{U-1} \sqrt{\frac{2E_{c,u}}{T_c}} \mathbf{H}_u \mathbf{C}_u d_u + \mathbf{N}, \quad (57)$$

where  $\mathbf{F}$  is the FFT matrix of size  $SF \times SF$ ,  $\mathbf{H}_u = \mathbf{F}\mathbf{h}_u\mathbf{F}^H$ ,  $\mathbf{N} = \mathbf{F}\mathbf{n}$ , and

$$\mathbf{C}_u = \mathbf{F}\mathbf{c}_u = \text{diag}\{1, \dots, e^{-j2\pi k u \Delta / SF}, \dots, e^{-j2\pi(SF-1)u\Delta/SF}\} \times \mathbf{C}. \quad (58)$$

In Eq. (58),  $\mathbf{C} = \mathbf{F}\mathbf{c}$  with  $\mathbf{c} = [c(0), \dots, c(t), \dots, c(SF - 1)]^T$ .  $\mathbf{C}$  is common to all  $U$  users ( $U \leq SF/\Delta$ ).

The  $u$ -th user is assumed to be the desired user. The  $u$ -th user's frequency-domain signal,  $\hat{\mathbf{R}}_u = [\hat{R}_u(0), \dots, \hat{R}_u(k), \dots, \hat{R}_u(SF - 1)]^T$ , after despreading and FDE can be written as

$$\hat{\mathbf{R}}_u = \mathbf{W}_u \mathbf{R} \quad (59)$$

with  $\mathbf{W}_u = \text{diag}\{W_u(0), \dots, W_u(k), \dots, W_u(SF - 1)\}$ . It can be understood from Eq. (57) that the  $u$ -th user's channel  $\mathbf{H}_u$  is altered to

$$\mathbf{H}_u \mathbf{C}_u = \text{diag}\{1, \dots, e^{-j2\pi k u \Delta / SF}, \dots, e^{-j2\pi(SF-1)u\Delta/SF}\} \times \mathbf{H}_u \mathbf{C}. \quad (60)$$

For clear understanding of the principle operation of DT/CDMA signal detection, we first consider the

frequency-domain despreading and the equalization separately. The frequency-domain despreading weight removes the spreading modulation and the cyclic time shift, but does not compensate for the distortion caused by the channel. The despreading weight is given as

$$W_u(k) = \left\{ C(k) \exp\left(-j2\pi k \frac{u\Delta}{SF}\right) \right\}^{-1}. \quad (61)$$

After despreading, the frequency-domain signal  $\hat{\mathbf{R}}$  is transformed by using an  $SF$ -point IFFT into the delay time-domain signal,  $\mathbf{y}_u = [y_u(0), \dots, y_u(\tau), \dots, y_u(SF - 1)]^T$ , as

$$\begin{aligned} \mathbf{y}_u &= \mathbf{F}^H \hat{\mathbf{R}}_u \\ &= \mathbf{F}^H \mathbf{W}_u \left( \sum_{u'=0}^{U-1} \sqrt{\frac{2E_{c,u'}}{T_c}} \mathbf{H}_{u'} \mathbf{C}_{u'} d_{u'} \right) + \mathbf{F}^H \mathbf{W}_u \mathbf{N}. \end{aligned} \quad (62)$$

From Eqs. (58) and (61), we have

$$\mathbf{W}_u \mathbf{H}_{u'} \mathbf{C}_{u'} = \begin{bmatrix} H_{u'}(0) \\ \vdots \\ H_{u'}(k) e^{-j2\pi k (u' - u) \Delta / SF} \\ \vdots \\ H_{u'}(SF - 1) e^{-j2\pi(SF-1)(u' - u) \Delta / SF} \end{bmatrix} \quad (63)$$

and therefore, Eq. (62) becomes

$$\begin{aligned} \mathbf{y}_u &= \sqrt{\frac{2E_{c,u}}{T_c}} \mathbf{F}^H [H_u(0), \dots, H_u(k), \dots, H_u(SF - 1)]^T d_u \\ &+ \sum_{\substack{u'=0 \\ \neq u}}^{U-1} \sqrt{\frac{2E_{c,u'}}{T_c}} \mathbf{F}^H \begin{bmatrix} H_{u'}(0) \\ \vdots \\ H_{u'}(k) e^{-j2\pi k (u' - u) \Delta / SF} \\ \vdots \\ H_{u'}(SF - 1) e^{-j2\pi(SF-1)(u' - u) \Delta / SF} \end{bmatrix} d_{u'} \\ &+ \mathbf{F}^H \mathbf{W}_u \mathbf{N}. \end{aligned} \quad (64)$$

The  $\tau$ -th element,  $y_u(\tau)$ , of  $\mathbf{y}_u$  is given by

$$\begin{aligned} y_u(\tau) &= \sqrt{\frac{2E_{c,u}}{T_c}} d_u h_u(\tau) \\ &+ \sum_{\substack{u'=0 \\ \neq u}}^{U-1} \sqrt{\frac{2E_{c,u'}}{T_c}} d_{u'} h_{u'}(\tau - (u' - u)\Delta) \\ &+ \frac{1}{\sqrt{SF}} \sum_{k=0}^{SF-1} \frac{N(k)}{C(k)} \exp\left(j2\pi k \frac{\tau + u\Delta}{SF}\right), \end{aligned} \quad (65)$$

where  $h_u(\tau)$  denotes the impulse response of the  $u$ -th user's channel given by

$$h_u(\tau) = \sum_{l=0}^{L-1} h_{u,l} \delta(\tau - \tau_l) \quad (66)$$

with  $h_{u,l}$  and  $\tau_{u,l}$  being the complex path gain and the time

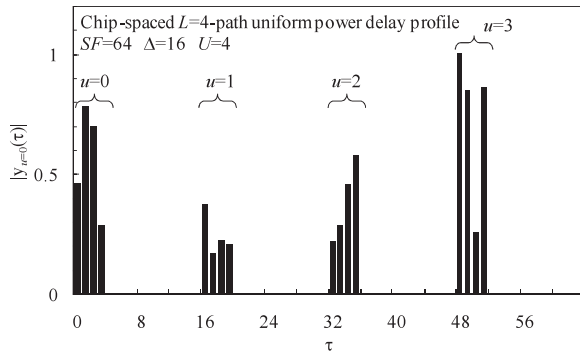


**Fig. 18** One shot observation of  $|y_{u=0}(\tau)|$  for an  $L = 4$ -path channel when  $U = 4$ .

delay of the  $l$ -th path for the  $u$ -th user, respectively.

It can be understood from Eqs. (65) and (66) that if  $\Delta$  is longer than or equal to the maximum time delay difference of the channel, the  $u$ -th user (desired user) signal component appears MAI-free in a delay-time interval of  $[0, \Delta - 1]$ . Figure 18 illustrates a one shot observation of  $U = 4$  users' signal components in  $|y_{u=0}(\tau)|$  when  $SF = 64$  for a channel having a chip-spaced  $L = 4$ -path uniform power delay profile. The decision variable  $\hat{d}_u$  can be obtained by using the coherent rake combining as

$$\begin{aligned} \hat{d}_u &= [h_u(0), \dots, h_u(\tau), \dots, h_u(\Delta - 1), 0, 0, \dots, 0]^* \mathbf{y}_u \\ &= \sum_{\tau=0}^{\Delta-1} h_u^*(\tau) y_u(\tau). \end{aligned} \quad (67)$$

The above coherent rake combining or equalization is equivalent to the MRC-FDE in the single-user environment.

It should be noted that the amplitude of  $C(k)$  is not constant and varies over  $k$  if a partial sequence of an  $SF$ -chip length taken from a long PN sequence is used as the spreading code. This causes the noise enhancement problem. If the Chu sequence [37], which has a constant amplitude, is used, the noise enhancement problem can be avoided. However, the number of Chu sequences is limited.

In [35], a new signal detection scheme is presented that can perform despreading, demultiplexing, and equalization simultaneously all in the frequency-domain. We derive the MMSE weight such that  $y_u(\tau)$  is as close to  $d_u \delta(\tau)$  as possible. The decision variable  $\hat{d}_u$  can be obtained as

$$\hat{d}_u = y_u(0) = \frac{1}{SF} \sum_{k=0}^{SF-1} \hat{R}_u(k). \quad (68)$$

The MMSE weight is used in order to extract the desired user's data-modulated symbol while reducing the MAI and noise (this means that the MAI remains at the cost of avoiding the noise enhancement problem), without transforming the frequency-domain signal into the delay time-domain signal. All of despreading, demultiplexing, and equalization are done simultaneously in the frequency-domain.

The Fourier transform of  $d_u \delta(\tau)$  is  $d_u$  for  $k = 0 \sim SF - 1$

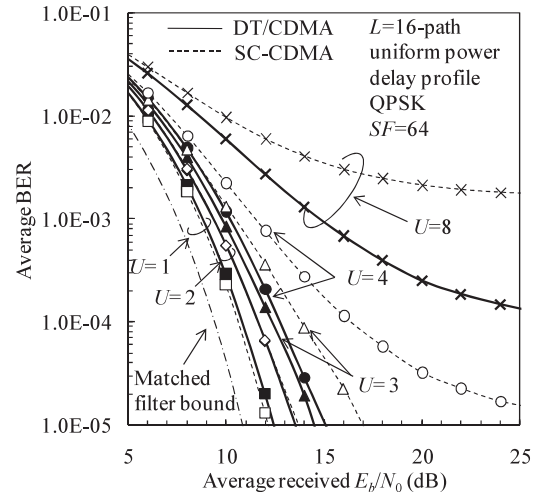


**Fig. 19** Uplink BER performance of DT/CDMA.

and the equalization error  $e(k)$  is defined as  $e(k) = \hat{R}_u(k) - d_u$ . Since data-modulated symbols of different users are independent, the one-tap MMSE weight is derived by solving  $\partial E[|e(k)|^2] / \partial W_u(k) = 0$  as

$$W_u(k) = \frac{\{C(k)H_u(k) \exp(-j2\pi k \frac{u\Delta}{SF})\}^*}{\frac{|C(k)|^2}{SF} \sum_{u'=0}^{U-1} \frac{E_{c,u'}}{N_0} |H_{u'}(k)|^2 + 1}. \quad (69)$$

Using the weight of Eq. (69) instead of Eq. (61), the phase variations in the received signal due to fading and spreading can be removed in the frequency-domain.

For the numerical evaluation of DT/CDMA performance, a frequency-selective block Rayleigh channel having a chip-spaced  $L = 16$ -path uniform power delay profile, i.e.,  $E[|h_{u,l}|^2] = 1/L$  and  $\tau_{u,l} = l$  for all  $u$ , is assumed. The spreading factor is set to  $SF = 64$ . The GI length is set to 16 chips; therefore,  $\Delta$  is set to  $\Delta = 16$  and the maximum number of uplink users to be multiplexed MAI-free is  $SF/\Delta = 4$ .

Figure 19 plots the uplink BER performance of the DT/CDMA as a function of the average received signal energy per bit-to-AWGN power spectrum density ratio  $E_b/N_0$  ( $= 0.5(E_{c,u}/N_0)(SF + \Delta)$ ), where we assume  $E_{c,u} = E_c$  for all  $u$ , i.e., slow TPC is applied. For comparison, the uplink BER performance of SC-CDMA with MMSE-FDE is also plotted. QPSK is used for data-modulation. Ideal channel estimation and ideal transmit timing control are assumed. The spreading code,  $\{c(t); t = nSF \sim (n+1)SF\}$ , for the  $n$ -th data-modulated symbol is taken from a long PN sequence with the repetition period of 4095 chips and shared by user  $u = 0$  to user  $u = 3$ . If  $U$  exceeds four but is less than eight (i.e.,  $SF/\Delta < U < 2(SF/\Delta)$ ), a different spreading code must be used for user  $u = 4$  to user  $u = 7$ ;  $\{c(t); t = (n+1)SF \sim (n+2)SF\}$  is used to spread the  $n$ -th data-modulated symbols of the user  $u = 4$  to user  $u = 7$ .

DT/CDMA using the MMSE weight given by Eq. (69) cannot completely remove the MAI since the orthogonality among different users is distorted to some extent and

therefore, the achievable BER performance degrades due to residual MAI as  $U$  increases. However, Fig. 19 shows that DT/CDMA provides better BER performance than SC-CDMA.

## 7. Conclusion

SC with FDE will play a very important role in future broadband wireless systems. In this article, after introducing the principle of joint FDE/antenna diversity combining, we introduced SC-FDMA, which has been adopted as the uplink multiple access scheme in the 3G LTE. We then introduced SC-CDMA and block spread CDMA. As another interesting multiple access scheme, DT/CDMA was introduced.

In future wireless systems, the distributed antenna system (DAS) or network (DAN) using SC with FDE may become a promising wireless access network. SC-DAN with FDE remains as an important future topic of study.

## References

- [1] F. Adachi, M. Sawahashi, and H. Suda, "Wideband DS-CDMA for next generation mobile communications systems," *IEEE Commun. Mag.*, vol.36, no.9, pp.56–69, Sept. 1998.
- [2] S. Hara and R. Prasad, "Overview of multicarrier CDMA," *IEEE Commun. Mag.*, vol.35, no.12, pp.126–133, Dec. 1997.
- [3] N. Yee, J.P. Linnartz, and G. Fettweis, "Multi-carrier CDMA in indoor wireless radio networks," *IEICE Trans. Commun.*, vol.E77-B, no.7, pp.900–904, July 1994.
- [4] E.A. Sourour and M. Nakagawa, "Performance of orthogonal multicarrier CDMA in a multipath fading channel," *IEEE Trans. Commun.*, vol.44, no.3, pp.356–367, March 1996.
- [5] H. Sari, G. Karam, and I. Jeanclaude, "An analysis of orthogonal frequency-division multiplexing for mobile radio applications," *Proc. 45th IEEE Veh. Technol. Conf. (VTC)*, vol.3, pp.1635–1639, June 1994.
- [6] H. Sari, G. Karam, and I. Jeanclaude, "Frequency-domain equalization of mobile radio and terrestrial broadcast channels," *IEEE Global Telecommunications Conference*, vol.1, pp.1–5, San Francisco, Nov.-Dec. 1994.
- [7] A. Czyliwik, "Comparison between adaptive OFDM and single carrier modulation with frequency domain equalization," *Proc. 47th IEEE Veh. Technol. Conf. (VTC)*, vol.2, pp.865–869, Phoenix, AZ, U.S.A., May 1997.
- [8] D. Falconer, S.L. Ariyavastakul, A. Benyamin-Seeyar, and B. Eidson, "Frequency domain equalization for single-carrier broadband wireless systems," *IEEE Commun. Mag.*, vol.40, no.4, pp.58–66, April 2002.
- [9] A.S. Madhukumar, F. Chin, Y.-C. Liang, and K. Yang, "Single-carrier cyclic prefix-assisted CDMA system with frequency domain equalization for high data rate transmission," *EURASIP J. Wireless Communications and Networking*, vol.2004, no.1, pp.149–160, Aug. 2004.
- [10] F. Adachi, D. Garg, S. Takaoka, and K. Takeda, "Broadband CDMA techniques," *IEEE Wireless Commun. Mag.*, vol.12, no.2, pp.8–18, April 2005.
- [11] C.-C. Hsieh and D.-S. Shiu, "Single carrier modulation with frequency domain equalization for intensity modulation-direct detection channels with intersymbol interference," *Proc. 17th IEEE International Symposium on Personal Indoor and Mobile Radio Communications (PIMRC)*, pp.1–5, Sept. 2006.
- [12] J.G. Proakis, *Digital Communications*, 4th ed., McGraw-Hill, 2001.
- [13] K. Takeda and F. Adachi, "Frequency-domain interchip interference cancellation for DS-CDMA downlink transmission," *IEEE Trans. Veh. Technol.*, vol.56, no.3, pp.1286–1294, May 2007.
- [14] M. Rohling, T. May, K. Bruninghaus, and R. Grunheid, "Broad-band OFDM radio transmission for multimedia applications," *Proc. IEEE*, vol.87, no.10, pp.1778–1789, Aug. 2002.
- [15] U. Sorger, I. De Broeck, and M. Schell, "Interleaved FDMA — A new spread-spectrum multiple-access scheme," *Proc. IEEE ICC98*, vol.2, pp.1013–1017, June 1998.
- [16] M. Schnell, I. Broeck, and U. Sorger, "A promising new wideband multiple-access scheme for future mobile communications systems," *European Trans. Telecommun. (ETT)*, vol.10, no.4, pp.417–427, July-Aug. 1999.
- [17] R. Dinis, D. Falconer, C.T. Lam, and M. Sabbaghian, "A multiple access scheme for the uplink of broadband wireless systems," *Proc. IEEE Globecom 2004*, pp.3808–3812, Dallas, Tx, U.S.A., Nov.-Dec. 2004.
- [18] H.G. Myung, J. Lim, and D.J. Goodman, "Single carrier FDMA for uplink wireless transmission," *IEEE Veh. Tech. Mag.*, vol.1, no.3, pp.30–38, Sept. 2006.
- [19] T. Frank, A. Klein, and E. Costa, "IFDMA: A scheme combining the advantages of OFDMA and CDMA," *IEEE Wireless Commun.*, vol.14, no.3, pp.9–17, June 2007.
- [20] D. Galda and H. Rohling, "A low complexity transmitter structure for OFDM-FDMA uplink systems," *Proc. IEEE 50th Veh. Technol. Conf. (VTC) Spring*, pp.1737–1741, May 2002.
- [21] 3GPP TR25.814, "Physical layer aspect for evolved universal terrestrial radio access (UTRA)," version 7.1.0.
- [22] Y. Goto, T. Kawamura, H. Atarashi, and M. Sawahashi, "Variable spreading and chip repetition factors (VSCRF)-CDMA in reverse link for broadband wireless access," *Proc. IEEE PIMRC2003*, vol.1, pp.254–259, Sept. 2003.
- [23] K. Takeda and F. Adachi, "Frequency-interleaved spread spectrum with MMSE frequency-domain equalization," *IEICE Trans. Commun.*, vol.E90-B, no.2, pp.260–268, Feb. 2007.
- [24] H. Fattah and C. Leung, "An overview of scheduling algorithms in wireless multimedia networks," *IEEE Wireless Commun.*, vol.9, no.5, pp.76–83, Oct. 2002.
- [25] J.Z. Haiying and R.H.M. Hafez, "Scheduling schemes for multimedia service in wireless OFDM systems," *IEEE Wireless Commun.*, vol.14, no.5, pp.99–105, Oct. 2007.
- [26] F. Adachi and K. Takeda, "Bit error rate analysis of DS-CDMA with joint frequency-domain equalization and antenna diversity combining," *IEICE Trans. Commun.*, vol.E87-B, no.10, pp.2991–3002, Oct. 2004.
- [27] X.D. Wang and H.V. Poor, "Iterative (turbo) soft interference cancellation and decoding for coded CDMA," *IEEE Trans. Commun.*, vol.47, no.7, pp.1046–1061, July 1999.
- [28] S. Zhou, G.B. Giannakis, and C.L. Martret, "Chip-interleaved block-spread code division multiple access," *IEEE Trans. Commun.*, vol.50, no.2, pp.235–248, Feb. 2002.
- [29] H. Atarashi, N. Maeda, Y. Kishiyama, and M. Sawahashi, "Broadband wireless access based on VSF-OFCDM and VSCRF-CDMA and its experiments," *European Trans. Telecommun.*, vol.15, no.3, pp.159–172, Jan. 2004.
- [30] F. Adachi, K. Ohno, A. Higashi, T. Dohi, and Y. Okumura, "Coherent multicarrier DS-CDMA mobile radio access," *IEICE Trans. Commun.*, vol.E79-B, no.9, pp.1316–1325, Sept. 1996.
- [31] K. Ohno and F. Adachi, "Reverse-link capacity and transmit power in a power-controlled cellular DS-CDMA system," *IEICE Trans. Commun. (Japanese Edition)*, vol.J79-B-II, no.1, pp.17–25, Jan. 1996.
- [32] L. Liu and F. Adachi, "2-dimensional OVSAF spread/chip-interleaved CDMA," *IEICE Trans. Commun.*, vol.E89-B, no.12, pp.3363–3375, Dec. 2006.
- [33] L. Hanzo, W. Webb, and T. Keller, *Single- and Multi-carrier Quadrature Amplitude Modulation*, Wiley, 2000.
- [34] F. Adachi, M. Sawahashi, and K. Okawa, "Tree-structured generation of orthogonal spreading code with different lengths for for-

ward link of DS-CDMA mobile radio," *Electron. Lett.*, vol.33, no.1, pp.27–28, Jan. 1997.

- [35] F. Adachi and K. Takeda, "Delay-time/code division multi-access in a frequency-selective channel," *Electron. Lett.*, vol.43, no.18, pp.984–986, Aug. 2007.
- [36] H. Harada and R. Prasad, "Cyclic extended spread coded multi-carrier CDMA/TDD transmission scheme for wireless broadband multimedia communications," *Proc. 48th IEEE Veh. Technol. Conf. (VTC)*, vol.3, pp.1899–1904, May 1998.
- [37] D.C. Chu, "Polyphase codes with good periodic correlation properties," *IEEE Trans. Inf. Theory*, vol.18, no.4, pp.531–532, July 1972.



**Fumi-yuki Adachi** received the B.S. and Dr.Eng. degrees in electrical engineering from Tohoku University, Sendai, Japan, in 1973 and 1984, respectively. In April 1973, he joined the Electrical Communications Laboratories of Nippon Telegraph & Telephone Corporation (now NTT) and conducted various types of research related to digital cellular mobile communications. From July 1992 to December 1999, he was with NTT Mobile Communications Network, Inc. (now NTT DoCoMo, Inc.), where he

led a research group on wideband/broadband CDMA wireless access for IMT-2000 and beyond. Since January 2000, he has been with Tohoku University, Sendai, Japan, where he is a Professor of Electrical and Communication Engineering at the Graduate School of Engineering. His research interests are in CDMA wireless access techniques, equalization, transmit/receive antenna diversity, MIMO, adaptive transmission, and channel coding, with particular application to broadband wireless communications systems. From October 1984 to September 1985, he was a United Kingdom SERC Visiting Research Fellow in the Department of Electrical Engineering and Electronics at Liverpool University. He was a co-recipient of the IEICE Transactions best paper of the year award 1996 and again 1998 and also a recipient of Achievement award 2003. He is an IEEE Fellow and was a co-recipient of the IEEE Vehicular Technology Transactions best paper of the year award 1980 and again 1990 and also a recipient of Avant Garde award 2000. He was a recipient of the Thomson Scientific Research Front Award 2004 and the Ericsson Telecommunications Award 2008.



**Hiromichi Tomeba** received his B.S., M.S., and Dr. Eng. degrees in communications engineering from Tohoku University, Sendai, Japan, in 2004, 2006, and 2008, respectively. Since 2006, he has been a Japan Society for the Promotion of Science (JSPS) research fellow. Currently he is a JSPS postdoctoral fellow at the Department of Electrical and Communications Engineering, Graduate School of Engineering, Tohoku University. His research interests include frequency-domain equalization and antenna diversity techniques for mobile communication systems. He was a recipient of the IEICE RCS (Radio Communication Systems) Active Research Award in 2004 and 2005.



**Kazuki Takeda** received his B.S. and M.S. degrees in communications engineering from Tohoku University, Sendai, Japan, in 2006 and 2008. Currently he is a Japan Society for the Promotion of Science (JSPS) research fellow, studying toward his PhD degree at the Department of Electrical and Communications Engineering, Graduate School of Engineering, Tohoku University. His research interests include precoding and channel equalization techniques for mobile communication systems.